SIMULATION OF THE EQUILIBRIUM OPERATION OF A CANDU REACTOR AND STUDIES OF THE COLLAPSING PROCEDURE IN THE FUEL MANAGEMENT DESIGN PROGRAM

by

Charles Olive, B.A. Sc.

PART B: McMASTER (OFF CAMPUS) PROJECT*

A report submitted to the School of Graduate Studies in partial fulfilment of the requirements for the degree of Master of Engineering

Department of Engineering Physics
McMaster University
Hamilton, Ontario, Canada

April, 1977

* one of two project reports; the other part is designated PART A: ON CAMPUS PROJECT

MASTER OF ENGINEERING (1977) McMASTER UNIVERSITY

Department of Engineering Physics Hamilton, Ontario

TITLE: Simulation of the Equilibrium Operation of a CANDU Reactor and Studies of the Collapsing Procedure in the Fuel Management Design Program

AUTHOR: Charles Olive, B.A. Sc. (U of T)

SUPERVISOR: Dr. O.A. Trojan

NUMBER OF PAGES: 80, vii

ACKNOWLEDGEMENTS

I would like to express my appreciation to Atomic Energy of Canada Limited, Power Projects, (Sheridan Park and Meadowvale) for allowing me to perform this study and for the use of their facilities.

Special thanks to Professor O.A. Trojan and Dr. A.L. Wight for their encouragement and supervision. To a large extent, this report is a result of the latter's informative suggestions and detailed review of the early drafts.

I greatly appreciate the help of Dr. D.G. Parkinson with whom I had several fruitful discussions and I am indebted to N.J. Abush and R.S. Sibley for their technical assistance which was particularly valuable at the beginning of the project when the computing facilities were unfamiliar.

Several of the passages in this report which describe the FMDP calculations are reproduced, with minor changes from the FMDP documentation.

Financial support from Atomic Energy of Canada Limited is gratefully acknowledged.

ABSTRACT

Estimates of fuel management data for the equilibrium operation of a specific CANDU reactor have been obtained by simulating a period of the reactor's history using the Fuel Management Design Program (FMDP).

The collapsing procedure in FMDP has been tested and improved. This procedure prepares a coarse mesh model of the reactor core from a detailed fine mesh calculation. The program calculates a set of coarse mesh parameters which, when used in the flux calculation, will regenerate exactly the same eigenvalue and flux distribution as the fine mesh model. These parameters can then be used with the coarse mesh, to calculate flux distributions for a series of perturbations from the reference calculation used in collapsing.

Several coarse mesh models were generated and studied. It was found that coarse mesh calculations with collapsed parameters result in large savings in computing costs compared to the same calculations with fine mesh, but with very little loss in accuracy.

TABLE OF CONTENTS

LIST OF TABLES

LIST OF FIGURES

1. INTRODUCTION

1.1 Project Objectives

This study had two objectives. The first was to simulate a period of operation of a specific CANDU reactor using the Fuel Management Design Program (FMDP) to obtain estimates of the following equilibrium data:

(i) the maximum channel and bundle powers,

(ii) the refuelling rate required to maintain criticality,

(iii) the average discharge bundle irradiation for the two regions (inner and outer core), and

(iv) fuelling power changes

The method of selection of channels for refuelling will be discussed.

The second objective was to test and improve the collapsing procedure in FMDP. A description of this procedure and its uses is given in Section 1.3 following an outline of the types of calculations which can be done with FMDP.

1.2 Description of FMDP

FMDP is a two group, three dimensional, neutron diffusion computer program designed to do a wide range of fuel management calculations for CANDU reactors. Reactor operation is simulated by computing flux distributions at a series of time steps. Irradiation

values for each fuel bundle in the core are increased at each time step using the current thermal flux. Cross sections for the flux calculation are obtained by interpolation in a table of cross sections as a function of irradiation. The tabulated cross sections are obtained from the lattice cell code POWDERPUFS-V[1].

The program is also capable of calculating flux distributions for a random distribution of fuel bundle burnups. This simulates a snapshot of a possible distribution of irradiation in the core at some possible instant during core life and will be referred to in this report as the instantaneous calculation. These calculations do not require a simulation of the previous history of the reactor.

In addition, the program does a time-averaged calculation. The code computes a flux distribution which is an average over a long period of equilibrium operation. This calculation also, does not require simulation of reactor history.

Details of these calculations are contained in Appendix A and in the FMDP documentation[2,3].

The method used by the code to simulate the reactor is described in Appendix B. Note that for the purpose of the flux calculation, the reactor can be modelled with fine mesh, normal mesh or coarse mesh as follows:

(i) In the fine mesh model each controller is represented by small mesh volumes of the order of the physical size of the device. This model contains a large number of mesh cells and the flux calculation is detailed, but expensive.

(ii) In the normal mesh model, the mesh planes coincide with the lattice cell planes, so that there is one mesh point per fuel bundle. The mesh cell size is one lattice pitch by 1 lattice pitch by 1 bundle length (1*1*1).

(iii) In the coarse mesh model, there are fewer than 1 mesh point per fuel bundle.

For the normal and coarse mesh models, incremental cross sections for the controllers can be smeared across the mesh cells by volume weight averaging, or can be generated using the collapsing procedure. This is described in the following section.

FMDP is still under active development. Each modification is identified by a version number indicating the date and status of the version. TST indicates a test version. ALW indicates that the version has been approved by A.L. Wight. The later versions should give better answers to the calculations.

Calculations in this study were done on the CDC 6600 computer located at the Chalk River Nuclear Laboratories. The operating system was SCOPE 3.4. Towards the end of the project some calculations were done on the newly installed CYBER 175 computer with the NOS/BE operating system. Jobs were submitted through terminals located at AECL Power Projects, Sheridan Park and Meadowvale.

1.3 Collapsing Procedure

The collapse module in FMDP prepares a normal or coarse mesh model of the reactor core from a detailed fine mesh reference calculation. The program calculates a set of normal or coarse mesh parameters which, when used in the flux calculation, will regenerate exactly the same eigenvalue and flux distribution as the fine mesh model. These parameters can then be used with normal or coarse mesh to calculate flux distributions for a series of perturbations from the reference case. The decreased number of mesh points with respect to fine mesh, results in lower computing costs. A penalty in terms of some loss in accuracy is incurred.

The proposed use of the collapsing procedure is illustrated by considering the study to optimize the fuel load of a CANDU reactor at startup with fresh and depleted fuel. The study requires the simulation of the reactor operation from startup with various initial fuel loads to onset of fuelling in 5 or 10 Full Power Day (FPD) steps. This period is of a transient nature and lasts for about 100 FPD. The initial fuel load is the configuration of natural and depleted fuel at startup. The objective of the study is to determine the UO_2 content of the depleted bundles and their location which give the most satisfactory reactor operation over the initial transient. A detailed discussion of this study is contained in Ref. 4.

The study can be done with FMDP using the following procedure:

(i) Generate a fine mesh reactor model.

(ii) Convert to a coarse mesh model using the collapsing procedure.

(iii) Run the simulation with coarse mesh for various initial core configurations. Select the optimum configuration.

(iv) Repeat the simulation with the optimum core configuration but with the fine mesh model.

Step (iv) gives the 'correct' answer for operation with the optimum core configuration.

The degree of coarseness which can be tolerated in step (iii) depends upon the difference in the fuel management data which are obtained for each initial core loading. This difference must be significantly greater than the error which results from using the coarse mesh model. The error must be known from previous testing of the collapsing procedure (step (iv) serves as a check on the error). For example, suppose the maximum bundle power over the initial transient with a particular initial loading is A kW. A second initial loading gives a maximum bundle power of B kW. The predicted percentage error in these values is C%. The coarse mesh model used to obtain X and Y is acceptable if $\frac{A - B}{(A + B)/2} \times 100$ is significantly greater than C.

The advantage of simulating operation with coarse mesh in step (iii) is in terms of reduced computing costs - the coarser the mesh used, the cheaper the study. Note that in the design of the larger CANDU reactors, fine mesh simulations become prohibitively expensive.

The collapsing procedure is as follows: The reference fine mesh distribution is volume weight averaged over the coarse mesh cells. A Σ_a and $\nu\Sigma_f$ is then calculated for each coarse mesh volume from

$$\nu\Sigma_f^{*} V\phi^2 = k(\Sigma_r^{1} V\phi^1 - \mathcal{L}^1) \qquad (1.3\text{-}1)$$

$$\Sigma_a^{*} V\phi^2 = (\Sigma_{1\rightarrow 2} V\phi^1 + \mathcal{L}^2) \qquad (1.3\text{-}2)$$

where

$\mathcal{L}^n = \sum_{i=1}^{6} b_i^n \phi_i^n$ is the sum of the coupling coefficients times the neighbouring fluxes,

ϕ^n is the cell volume averaged flux in group n(n = 1,2),

$\nu\Sigma_f^*$, Σ_a^* are the fission source and thermal absorption cross-sections which will reproduce the given flux distribution,

Σr^1 is the group removal cross section,

$(\Sigma_r^1 = \Sigma_a^1 + \Sigma_{1\rightarrow 2})$, $\Sigma_{1\rightarrow 2}$ is the group 1 to 2 transfer cross-section, and

k is the fine mesh eigenvalue.

Note that these are simply the seven point finite difference two group diffusion equations rearranged to solve for the unknown cross-sections with a given flux distribution.

The program then generates and stores the set of cross-section increments for further use. Thus

$$\Delta\nu\Sigma_f = \nu\Sigma_f^* - \nu\Sigma_f \qquad (1.3\text{-}3)$$

$$\Delta\Sigma_a = \Sigma_a^* - \Sigma_a \qquad (1.3\text{-}4)$$

The $\nu\Sigma_f$ and Σ_a are the normal cell cross-sections unperturbed by an absorber.

The fine mesh reference flux distribution can be generated with a time-averaged calculation to produce time-averaged collapsed parameters, or by the instantaneous calculation to produce instantaneous collapsed parameters.

By way of example, consider the simplified section of a core shown modelled in fine mesh in Fig. 1a. It consists of one lattice cell, perturbed by a thermal absorber. One mesh point is at the centre of each of three fine mesh cells. Suppose we want to generate the normal mesh model. The normal mesh boundaries are shown in Fig. 1b and coincide with the lattice cell boundaries. In preparation for collapsing, a set of normal mesh cross-sections are calculated for the normal mesh cell; the thermal cross-sections are $\bar{\Sigma}_a = \Sigma_a^{MODERATOR} + \Sigma_a^{FUEL}$ and $\nu\bar{\Sigma}_f = \nu\Sigma_f^{FUEL}$ where the fuel cross-sections are previously calculated by the lattice cell code by flux volume weight averaging. Note that the effect of the absorber is not included in these smeared cross-sections.

The next step is to generate a fine mesh reference flux distribution and eigenvalue. For the section of the core considered, there will be three values for the fast flux ($\phi^1_{CELL\ 1}$, $\phi^1_{CELL\ 2}$, $\phi^1_{CELL\ 3}$) and three values for the thermal flux ($\phi^2_{CELL\ 1}$, $\phi^2_{CELL\ 2}$, $\phi^2_{CELL\ 3}$).

The fine mesh flux distributions are collapsed to normal mesh by volume weight averaging

i.e. $$\phi^1_{NM} = \frac{V_1\phi^1_{CELL\ 1} + V_2\phi^1_{CELL\ 2} + V_3\phi^1_{CELL\ 3}}{V}$$

and $$\phi^2_{NM} = \frac{V_1\phi^2_{CELL\ 1} + V_2\phi^2_{CELL\ 2} + V_3\phi^2_{CELL\ 3}}{V}$$

ϕ^1_{NM} and ϕ^2_{NM} are the fluxes, perturbed by the absorber, at the centre of the normal mesh cell. V_1, V_2 and V_3 are the volumes of the fine mesh cells, and V is the normal mesh volume.

The next step is to adjust two of the normal mesh cross-sections so that, when the diffusion equations are solved for our normal mesh cell, ϕ^1_{NM} and ϕ^2_{NM} will result. Most of the devices which are added to the core are strong thermal absorbers which strongly perturb the thermal flux distribution. For this reason the two thermal cross-sections ($\nu\Sigma_f$ and Σ_a) are most affected and were selected as the adjusted cross-sections.

Thus for the cell in Fig. 1b,

$$\nu\Sigma_f^{*} \, V\phi_{NM}^{2} = k(\Sigma_r^{1} \, V\phi^{1}_{NM} - \mathcal{L}^{1})$$

and

$$\Sigma_a^{*} \, V\phi^{2}_{NM} = (\Sigma_{1\rightarrow 2} \, V\phi^{1}_{NM} + \mathcal{L}^{1}) \quad .$$

The cross sectional increments are then generated (Eq. 1.3-3 and 1.3-4) and stored for use in perturbation calculations.

A normal mesh model can also be generated by simple smearing of the absorber cross-section across the normal mesh cell. (The fine mesh model is not required for this.)

i.e. $$\Delta\Sigma_{aNM}^{ABSORBER} = \frac{V_2 \, \Sigma_a^{ABSORBER}}{V}$$

where

$\Sigma_a^{ABSORBER}$ is the cross-section of the pure absorber, and

$\Delta\Sigma_{aNM}^{ABSORBER}$ is the smeared cross section for the cell.

However, when used in the unperturbed flux calculation the correct, collapsed reference values will not be regenerated. Perturbation calculations with a model generated by this procedure were not done in this study. The calculations will presumably be less accurate than when the same coarse mesh is used but with parameters generated by the collapsing procedure.

1.4 Description of Reactor

The reactor modelled in this study, is a right circular cylinder lying on its side and containing 480 horizontal fuel channels of which 208 are in the inner (high burnup) region and 272 are in the outer region. There are 13 bundles per channel of which 12 are in the active core. One half of a bundle at each end of the channel is outside the core. Refuelling occurs on power and is bidirectional. The reference refuelling scheme is eight bundle shift. The reactor is moderated and cooled with heavy water. Full core power is 2695 MW thermal to coolant. Spatial control is by vertical, light water zone controllers.

1.5 Previous FMDP Studies

The fine mesh model of D.G. Parkinson[5] was used in this study. The mesh spacings for half core symmetry are shown in Fig. 2. Average discharge irradiations of 1.78 n/kb for the inner region and 1.50 n/kb for the outer region were obtained from an eight bundle shift time-averaged calculation. This calculation was used as a reference throughout this project. The channel power distribution is shown in Fig. 3 and the bundle powers for eight specific channels are shown in Fig. 4.

A representative set of instantaneous power distributions have been obtained by D.G. Parkinson[5]. One of these was used in the preliminary testing of the collapsing procedure.

2. INVESTIGATION OF THE COLLAPSING PROCEDURE

2.1 CP Factor Improvement

The first two collapsed parameters ($\Delta\Sigma_a$ and $\Delta\nu\Sigma_f$) when used for the reference flux calculation with coarse mesh, exactly regenerate the same eigenvalue and flux distribution as the fine mesh model. However, the bundle power distribution is of more interest in fuel management studies. To regenerate the correct reference power distribution, a third collapsed parameter is required. Before this can be defined, the procedure used to calculate the bundle powers must be described.

This procedure is as follows. The thermal flux distribution obtained by the iterative solution of the diffusion equations, is volume weight averaged over the lattice cell array generating the unnormalized cell flux array, CELLFLUX. The unnormalized power is then computed for each bundle using the following equation:

$$\text{POWER} = \text{CELLFLUX} * \text{H FACTOR} \qquad (2.1\text{-}1)$$

where the conversion factor, H Factor, is a tabulated function of the bundle irradiation obtained from POWDERPUFS-V. Powers and fluxes are then normalized using the core design thermal power to coolant.

The cell fluxes, and hence the bundle powers, which result from volume weight averaging the reference coarse mesh flux distribution are not the same as result from volume weight averaging the reference fine mesh distribution. This can be seen from the series of figures on Page 49.

Fig. 5a shows the reference (time-averaged) thermal flux distribution along channel D-4. Each point is the flux at the centre of a fine mesh cell. The open circles mark the coarse mesh values obtained after collapsing the fine mesh distribution to 1*1*4 cell size (see Fig. 6). Note that for this particular channel, the fine mesh, coarse mesh, and lattice cell boundaries coincide in the radial (x and y) direction and differ only in the axial (z) direction. This is not generally the case with other channels, and D-4 was chosen as an example to simplify the discussion. Volume weight averaging is required only in the axial direction.

Fig. 5b shows the cell flux distribution along D-4 which results after volume weight averaging the coarse mesh distribution over the lattice cells. These fluxes, when used in Eq. 2.1-1 do not generate the correct bundle powers for channel D-4.

The third collapsed parameter can now be defined:

$$\text{CP FACTOR} = \frac{\text{CELL FLUX}^{FM}}{\text{CELL FLUX}^{CM}} \quad \text{at each lattice cell} \qquad (2.2\text{-}2)$$

CELL FLUX^{FM} is the cell flux generated by the fine mesh reference flux distribution (Fig. 5b), and

CELL FLUX^{CM} is the cell flux generated by the coarse mesh flux distribution (Fig. 5c).

The CP FACTORS for channel D-4 which would be obtained from this particular reference fine mesh flux distribution and coarse mesh cell size, are shown in Fig. 5d. These would be used in subsequent perturbation calculations with coarse mesh 1*1*4 to give a better estimate of the bundle power distribution. This occurs after the perturbed cell fluxes are adjusted using the following equation:

Adjusted CELL FLUX = CELL FLUX*CP FACTOR at each lattice cell.

The increase in computing costs to generate, store and use the CP FACTOR array is negligible.

2.2 Preliminary Testing

Preliminary testing of the collapsing procedure was carried out as follows:

(i) A half core instantaneous calculation with NRAN = 6389 (see Appendix A) was done with fine mesh

(ii) Time-averaged collapsed parameters (the $\Delta\Sigma_a$ and $\Delta V\Sigma_f$ of Eqs. 1.3-3 and 1.3-4 and the CP FACTORS of Eq. 2.2-2) were obtained by collapsing the time-averaged fine mesh calculation to coarse mesh.

(iii) The instantaneous calculation of step (i) was repeated with the coarse mesh model of step (ii). The power and cell flux distributions were compared with the 'correct' distributions of step (i) using the analyze module in FMDP. This computed the ratio of each element in the distributions from the coarse mesh calculation to the corresponding element from the fine mesh distribution. The average ratio and the standard deviation were then calculated. The latter is a measure of the accuracy of the coarse mesh distribution - the larger it is the greater the inaccuracy and, assuming an average ratio of unity, the higher the maximum error.

Steps (ii) and (iii) were done for a series of coarse mesh, half core geometries. These are shown in Fig. 6.

Results of Preliminary Testing

Important data from the fine mesh instantaneous calculation are tabulated in Table 2. The calculation was done twice; with version JUN1776TST and with version DEC0176ALW about 6 months later. The answers obtained were significantly different. The reason for this inconsistency has not been determined. Note, however, that there was minimal difference in the time-averaged calculations with versions JUN1776TST and SEP0176ALW (Table 1).

Statistical comparison with time-averaged data is contained in Table 3. The standard deviation here is a measure of the degree of perturbation. Additional comparison of the channel powers, in Fig. 7 showed a mean difference from time-averaged values of 11.5 percent.

The effect of the CP FACTORS on the accuracy of the 1*1*6 calculation is shown in Fig. 8. The bundle powers along channel D-12 from the coarse mesh calculation with and without the CP FACTORS are compared with the fine mesh powers obtained from version JUN1776TST. The accuracy was considerably increased when the factors were used.

Results from the instantaneous calculation with 5 coarse mesh models are presented in Table 4. Note that the calculation with normal mesh (case 1*1*1) was done without the CP FACTOR improvement to be consistant with the normal mesh simulation described in the next section. This simulation was started before the program changes were ready.

Comparison with the fine mesh result is contained in Table 5. Case 1*1*1, run with version JUN1776TST, was compared with the JUN1776TST fine mesh calculation, while cases 1*1*2, 1*1*4, 1*1*6 and 2*2*2 run much later in the project, were compared with the DEC0176ALW fine mesh calculation.

The results show that, of the coarse mesh calculations done, the most accurate answer is obtained from case 1*1*2. The channel power distribution for case 1*1*1 is second in order of accuracy, but the 1*1*1 bundle and cell flux distributions are a little less accurate than the distributions for case 1*1*4. If case 1*1*1 were repeated with the CP FACTOR improvement, it would presumably give the most accurate results (i.e. closest to the fine mesh results). Of the coarse mesh models tested, the normal mesh model contains the largest number of mesh cells.

Note that all distributions for case 2*2*2, in which the reactor is modelled with 1440 mesh points, were closer to fine mesh than the 1*1*6 (with 2720 mesh points) distributions. Also, the maximum channel and bundle power and k_{eff} were more accurate in the former calculation. An explanation of this result is as follows. Suppose the error in the flux calculated at each coarse mesh cell is a function of the mesh spacings, and that this function is separable in the X,Y and Z directions:

$$\text{i.e. Error} = C_1\Delta X^n + C_2\Delta Y^m + C_3\Delta Z^p \qquad (2.2\text{-}1)$$

If the constants and powers have roughly the same value.

$$\text{Error} \approx C_1(\Delta X^n + \Delta Y^n + \Delta Z^n)$$

For cell size 1*1*6, $\Delta X = 28.575$, $\Delta Y = 28.575$, $\Delta Z = 297.18$
For cell size 2*2*2, $\Delta X = 57.15$, $\Delta Y = 57.15$, $\Delta Z = 99.06$

$$\therefore \frac{\text{Error}_{2*2*2}}{\text{Error}_{1*1*6}} = \frac{57.15^n + 57.15^n + 99.06^n}{28.575^n + 28.575^n + 297.18^n}$$

For positive values of n greater than .25, this ratio is less than 1 and the flux calculated for a cell with 2*2*2 dimensional is the more accurate.

The bundle powers obtained in specific channels, including D-12 which has the maximum value, are compared in Figs. 9 and 10. The percentage error is indicated after each value. Consider Fig.10 Most of the bundle powers calculated with coarse mesh in D-12 are slightly lower and closer to the time-averaged (reference) values. For example, consider bundle D-12, No. 5. The reference power is 685.1 kW (see Fig.4). The instantaneous power calculated with fine mesh is 883.5 kW. This is a 29.0 percent perturbation from reference. The instantaneous powers calculated with 1*1*2, 1*1*4, 1*1*6. 2*2*2 cell size are 883.1 (28.9), 878.7 (28.3), 861.6 (25.8), and 867.7 kW (26.7) respectively. The degree of perturbation from reference indicated,in parentheses after each value,is decreased for each coarse mesh case and for the 1*1*n series of geometries, decreases with increasing cell size.

Now consider channel Q-1 which has a high negative perturbation from reference. The bundle powers calculated with coarse mesh are generally greater than when calculated with fine mesh and, again, the degree of perturbation from reference generally decreases with increasing cell size.

These results apply to most of the bundle and powers, but not all. They are explained by the following hypothesis:

The degree of perturbation of an instantaneous calculation is generally reduced slightly when the calculation is done with coarse mesh using time-averaged collapsed parameters.

Note also that the excess reactivity obtained with coarse mesh is low and closer to the time-averaged value in all cases (see Table 4). This further supports the above hypothesis.

A 4*4*4 coarse mesh model was also generated. The instantaneous flux calculation did not converge. The incremental cross-sections

were printed so that the adjusted thermal cross-sections used in the flux calculation could be determined at various mesh points. It was found that at some mesh points, particularly at the core edge, a negative adjusted cross-section resulted. It was concluded that there is a limit in coarseness to the collapsing procedure which is exceeded by the 4*4*4 model.

2.3 Accuracy of coarse mesh simulations with Collapsed Parameters

The error in the power and flux distributions and excess reactivity obtained with a specific coarse mesh model at some time in a simulation, is compounded of two factors. These are:

(i) The degree of perturbation from the fine mesh flux distributions and eigenvalue used in collapsing, and

(ii) The error in the bundle irradiation distribution.

The first factor is investigated using the instantaneous calculation with the procedure of the previous section. The second is discussed below.

Consider a simulation with fine mesh. When the first time step is taken, the bundle irradiation array is incremented using the bundle flux and F factor from the initial flux calculation as shown in the following equation.

$$\omega_K^{FM}(t_1) = \omega_K^{FM}(t_o) + f_K^{FM}(\omega_o)\phi_{Ko}^{FM}\Delta t_1 \quad \text{for bundle K} \qquad (2.3\text{-}1)$$

The superscript indicates the fine mesh reactor model. The nomenclature is provided in Appendix A.

The corresponding equation for the reactor modelled in coarse mesh with collapsed parameters is

$$\omega_K^{CM}(t_1) = \omega_K^{CM}(t_o) + f_K^{CM}(\omega_o)\phi_{Ko}^{CM}\Delta t_1 \qquad (2.3\text{-}2)$$

For the same starting conditions

$$\omega_K^{FM}(t_o) = \omega_K^{CM}(t_o)$$

$$f_K^{FM}(\omega_o) = f_K^{CM}(t_o)$$

$$\phi_{Ko}^{FM} = \phi_{Ko}^{CM} + \delta\phi_K^1$$

$\delta\phi_K^1$ is the error in the bundle flux from the coarse mesh calculation with respect to the bundle flux calculated with fine mesh. For a particular coarse mesh geometry, this error depends upon the perturbation of the first flux distribution from the fine mesh flux distribution used in collapsing. If there is no perturbation, $\delta\phi_1$ is zero. The error in the irradiation of bundle K after the first time-step is therefore $\delta\phi_K^1 f_K^{CM}(\omega_o)\Delta t_1$ and the lattice cell cross-sections, computed from fuel tables, for the coarse mesh flux calculation at t_1 will not be the same as those obtained for the fine mesh model.

After n times steps, the error in the irradiation at bundle K is $\delta\phi_K^1 f_K(\omega_o)\Delta t_1 + \delta\phi_K^2 f_K(\omega_1)\Delta t_2 + \ldots\ldots + \delta\phi_K^n f_K(\omega_{n-1})\Delta t_n$.

Note that the error in the F-factor, a weak function of irradiation, has been taken as negligible at each time-step. Note also that the number of error terms at each bundle location does not increase indefinitely. When the channel is refuelled and bundle K is replaced with a fresh bundle the error at this location becomes zero. (This is, of course, provided that the fuelling schedules for fine mesh and coarse mesh simulations are the same) The irradiation of each refuelled bundle is known exactly (i.e. 0.0 n/kb).

The irradiation distributions from a coarse mesh simulation can be compared, at each time step, with the exact fine mesh answer. Since $\delta\phi$ is as likely to be positive as negative, it is expected that the average ratio at each time step will be unity. i.e.

$$\sum_{K=0}^{m}\left(\frac{\omega_K^{CM}\big|_t}{\omega_K^{FM}\big|_t}\right)_m = 1$$

where m = number of bundles in core.

However, the standard deviation and maximum error would increase with time and approach steady state values. After a long period of simulation (greater than the average residence time of bundles in the core) the maximum error will always occur at a bundle location with the maximum (or close to) number of error terms.

To investigate the above rigorously, a fine mesh reference simulation is required, followed by the same simulation with a series of coarse mesh reactor models. Unfortunately, the full core fine mesh model required more central memory than was available at the time. The reference simulation was done with normal mesh. Time-averaged collapsed parameters (without CP FACTORS) were generated for normal mesh geometry (see Fig. 6) using the half core fine mesh model, and unfolded to full core. Start conditions were generated by the instantaneous module with a "patterned channel age distribution" (see Appendix A). This reduced power tilts and the clustering of channels with fresh fuel to a minimum and, hence, the initial core conditions could be regarded as optimized. The simulation proceeded for 70 Full Power Days (FPD) with a 5 or 10 FPD step between each flux calculation. Criticality was maintained with the manual refuelling procedure described in Sect. 3.2. Each zone controller was kept at 40 percent fill.

The simulation was repeated with two other coarse mesh geometries (1*1*4 and 1*1*6 cell size) and started for a third (2*2*2). Time-averaged collapsed parameters, including the CP FACTOR arrays, were used. The irradiation distributions were compared at each time step with the distributions generated with the normal mesh model.

Comparison of Simulation Data

The simulation data are compared in this section. A detailed discussion of the normal mesh simulation is contained in Sect. 3.

For convenience, the starting point for each simulation has been set to 0 FPD. Only one flux calculation was done at 0 FPD. This was for the normal mesh simulation. The coarser mesh simulations were started not only with the same irradiation distribution, but also with the same bundle and flux distributions. It would have been better to do the flux calculation at 0 FPD for each case. The burns for the first time step are identical.

Tables 6, 7 and 8 show respectively the bulk excess reactivity and the maximum channel and bundle powers, with location, for each simulation as a function of time. Although there is very little difference in the values at each time step, the order of accuracy was predicted from the instantaneous calculations of Sect. 2.2. Note, however, that the maximum powers obtained at the first flux calculation with 2*2*2 cell size seem less accurate than the 1*1*6 values (taking the 1*1*1 channel powers and 1*1*4 bundle powers to be the closest to the fine mesh answers) and are probably greater than the fine mesh result.

Average irradiations of bundles discharged in 4 specific timesteps are compared in Table 9. The values increase with increasing mesh coarseness and, as expected, the difference increases slightly with time.

The power and cell flux distributions were compared at four specific times in the simulation and the irradiation distributions were compared at every time step. These results are shown in Table 10 and Fig. 11. The difference in channel power and irradiation distributions increases with time as expected, although the difference in the bundle power distributions remains fairly constant. The average irradiation ratio at each time step was not unity but decreased with time. The reason for this may be because the CP Factor array was not used in the reference simulation, but was used for the other two cases. If a fine mesh simulation becomes possible, the analysis should be repeated with the fine mesh answer as reference.

Simulation results for 5 specific channels are presented in Figs. 12 to 36 permitting absolute comparison of the data. The percentage difference from reference is indicated after each value.

2.4 Cost Analysis

Sect. 2.2 and 2.3 have determined the loss in accuracy which results from Fuel Management calculations with normal and coarse mesh reactor models generated by the collapsing procedure in FMDP. The purpose of this subsection is to estimate the savings which result from lower computing costs.

The following equation has been used, until quite recently, by the computing centre for costing jobs

$$\text{Cost}^{8} \text{ in } \$ = \frac{0.29}{0.28}\left[0.293*CP + 0.109*I\emptyset + 0.408*10^{-4}*(CP + I\emptyset)*(\text{avg CM})^{2}\right] \qquad (2.4\text{-}1)$$

where avg CM $= i\,\frac{\Sigma(0.001CP + 0.001I\emptyset)}{CP + I\emptyset}\,Fl_i$ kilowords

FMDP periodically writes to output current memory and CP and IØ times during the execution of a module so that a value for each of these parameters can be estimated for each subcomputation within the module. The costing equation can then be applied to each subcomputation. This allows a more complete indication of the savings (and where they occur) for the calculations with coarse mesh.

Results

The breakdown of the system requirements and costs for the various computations and core models are given in Tables 11 and 12. The system requirements are based on version DEC0176ALW and the costs were calculated using equation 2.4-1. Note the following:

The value of the CP time for the flux calculation (in millisecs per iteration per mesh point) was the average over 14 runs done during November and December 1976 on the CDC 6600 computer. The standard deviation was 0.0102.

The average CM for some of the computations was sometimes difficult to determine without detailed examination of the coding. The values recorded are the author's best estimate from the current CM which is periodically written to output during a job. The values for the flux calculation are, however, exact except for the full core fine mesh which, before reaching this step, exceeded the system CM available.

Total costs for various jobs were determined using Tables 11 and 12, and are shown in Table 13. Average CP and IØ times were used for reading data from tape to mass storage at the start of each job and for writing back to tape at the end. Note, however, that with coarse mesh there is less data than with fine mesh resulting in lower costs. This saving is not reflected in Table 18 but is relatively small. The fine mesh half core instantaneous calculation was about 2-1/2 times the cost of the calculation with 2*2*2 mesh.

FMDP uses considerable amounts of extended core storage. The maximum is printed at the end of each job. Less ECS is used with coarse mesh so that savings would be greater than shown in Table 18 if there had been a charge for ECS.

A particular job was broken down into its components and the total cost estimated using the above procedure, but with the actual CP and IØ times for the flux calculation and for reading from and writing to tape. The answer agreed to within 4 percent of the cost for the job listed in the monthly statement.

2.5 Further Testing of the Collapsing Procedure

2.5.1 Instantaneous Collapsed Parameters

This study has examined the loss in accuracy and savings in cost for calculations with time-averaged collapsed parameters for various coarse meshes. FMDP also provides for the generation and use

of instantaneous collapsed parameters. For a simulation, these would be generated using the fluxes and eigenvalue from the fine mesh calculation with the start reactor conditions. The initial power distribution from the coarse mesh calculation is exactly the same as the distribution from the fine mesh calculation. It is therefore more accurate than the initial distribution obtained with time-averaged parameters. As the simulation proceeds and the irradiation distribution differs more and more from the initial distribution, the accuracy will decrease and eventually become less than the accuracy obtained with time-averaged parameters. However, a new set of instantaneous parameters can be generated periodically by a fine mesh calculation with the current reactor conditions.

2.5.2 Compound Incremental Cross-sections

The effect of a thermal absorber on the thermal cross-sections is increased in regions of high thermal flux and decreased in regions of low thermal flux. This means that, for each cell,

$$\text{when } \phi^P > \phi^R, \quad \left|\Delta\nu\Sigma_f{}^P\right| > \left|\Delta\nu\Sigma_f{}^R\right| \text{ and}$$

$$\left|\Delta\Sigma_a{}^P\right| > \left|\Delta\Sigma_a{}^R\right|$$

$$\text{and when } \phi^P < \phi^R, \quad \left|\Delta\nu\Sigma_f{}^P\right| < \left|\Delta\nu\Sigma_f{}^R\right| \text{ and}$$

$$\left|\Delta\Sigma_a{}^P\right| < \left|\Delta\Sigma_a{}^R\right|$$

The subscript indicates that the value is for the perturbation or reference calculation.

The cell flux will generally be greater than the time-averaged value if the cell contains fresh fuel and less than the time-averaged value if the fuel is high burnup. (This may not be the case with extreme cell boundary conditions). This means that generally the following conditions hold:

when $\phi^P > \phi^R$, $\Sigma_a{}^P < \Sigma_a{}^R$ and

$$\nu\Sigma_f{}^P > \nu\Sigma_f{}^R$$

and when $\phi^P < \phi^R$, $\Sigma_a{}^P > \Sigma_a{}^R$ and

$$\nu\Sigma_f{}^P < \nu\Sigma_f{}^R$$

The incremental cross-sections from the absorber can be made dependent upon cell conditions by storing compound incremental cross-sections. These are $\Sigma_a{}^R$, $\Delta\Sigma_a{}^R$ and $\dfrac{\Delta\nu\Sigma_f{}^R}{\nu\Sigma_f{}^R}$. $\Sigma_a{}^R$ and $\nu\Sigma_f{}^R$ are the coarse mesh reference cross-sections unperturbed by the absorber. $\Delta\Sigma_a{}^R$ and $\Delta\nu\Sigma_f{}^R$ are the incremental cross-sections generated in the normal way by the collapsing procedure.

The incremental cross-sections for a particular perturbation calculation are generated as follows:

$$\Delta\Sigma_a{}^P = \frac{\Sigma_a{}^R}{\Sigma_a{}^P} \cdot \Delta\Sigma_a{}^R \qquad (2.5\text{-}1)$$

and

$$\Delta\nu\Sigma_f{}^P = \frac{\Delta\nu\Sigma_f{}^R \; \nu\Sigma_f{}^P}{\nu\Sigma_f{}^R} \quad . \qquad (2.5\text{-}2)$$

3. DISCUSSION OF NORMAL MESH SIMULATION

3.1 Fuelling Objectives

After each flux calcuation, the irradiation and channel power distributions were used in the selection of channels for refuelling in the next time step. Channels were selected in order to achieve the following objectives:

(i) Minimize the maximum ratio of channel power to reference (time-averaged) channel power. This is abbreviated to"maximum channel overpower" in this report and is expressed as a percentage. Since the reference power distribution is normally used to set channel flow rates, this parameter is an indication of channel outlet temperature or outlet quality if the channel is boiling. It is desirable to keep the channel overpower low in order to minimize problems associated with boiling in the channels.

(ii) Minimize the maximum bundle power. To reduce fuel defects, fuel element centre temperatures and fission gas pressure, it is desirable to keep fuel rating low. The total power which can be obtained from the core is limited by this parameter.

(iii) Minimize the fuelling rate which keeps the reactor critical.

3.2 Fuelling Rules

To achieve the third objective, preference was given to the oldest channels. Channel ages were calculated at each time step using Eq. 3.2-1.

$$\text{CHANNEL AGE} = \frac{\text{AVERAGE IRRADIATION OF THE 8 BUNDLES WHICH ARE DISCHARGED WHEN CHANNEL IS FUELLED}}{\text{TIME AVERAGED EXIT IRRADIATION}} \qquad (3.2\text{-}1)$$

The two major reasons for high channel overpowers are as follows:

(i) The channel effect; the bundle power per unit flux varies with time. The power increases in a natural uranium bundle owing to plutonium buildup and then decreases until the minimum is reached at the time of refuelling.

(ii) The local effect; the channel effect will be amplified if a channel is refuelled in a region that tends to show a clustering of fresh channels. P. Stevens[7] obtained a relationship between the additional increase in power for a channel and the average burnup of the eight neighbouring channels.

When a channel was refuelled in the simulation, one of its neighbours was refuelled only after the core burnup had increased by at least 15 FPD to minimize the local effect.

To keep a uniform power distribution throughout the simulation, the core was divided radially into seven zones (Fig. 3). At each time step, the ratio of each zonal power to the corresponding time-averaged

zonal power was calculated. Channels were selected for refuelling in the subsequent timestep in an attempt to obtain ratio values of unity for each zone. The fuelling rate in a zone with a ratio of less than 1 was increased, and decreased when the ratio was greater than 1.

3.3 Simulation Results

Fig. 37 shows the excess reactivity plotted against core burnup. The excess reactivity changes linearly with burnup for each step because of uniform refuelling.

The equilibrium fuelling rate, averaged over 70 FPD was 2.821 channels per FPD. This is an adjusted value to allow for the difference in excess reactivity at the start and end of the simulation. An excess reactivity decrease of 0.417 milli-k per FPD in the absence of fuelling was assumed.

The average discharge irradiations for outer and inner core bundles were 1.506 and 1.775 n/kb respectively. These are within 1/2 percent of the values obtained from the time-averaged calculation.

Maximum bundle and channel powers were 874 kW and 7100 kW respectively. The maximum channel overpower (12.5%) occured in the outer core at channel A-14 (see Table 14).

The above data are summarized in Table 15.

An example of fuelling is given in Fig. 39 which shows the channels chosen for fuelling in the interval 30 to 40 FPD. Each selected channel is marked with a 'X' and the age and power of the eight neighbouring channels at 30 FPD have been recorded. The complete fuelling history is contained in Appendix C.

Zonal overpowers, overall power tilts and the fuelling history by zones are recorded in Table 16. The maximum zonal overpower was 6 percent and occured in zone 3 at 20 FPD. The top to bottom power tilt at this time was 3.24 percent. No channels were fuelled in zone 3 in the next burnup interval and the zonal overpower decreased to -4.4 percent at the next flux calculation.

Note that the simulation was somewhat short to reliably estimate the maximum powers and the fuelling rate to be expected during equilibrium operation. The simulation should be continued to about 150 FPD.

3.4 Analysis of Simulation Results

The following is an attempt to identify the cause or causes of the maximum channel power and overpower which result at 60 FPD. First note that:

(i) the maximum channel power was 7091 kW occuring at 0-8 in the adjusted region.

(ii) the maximum channel overpower was 10.75 percent occuring at 0-7 also in the adjusted region. 0-7 was refuelled at 56 FPD.

(iii) channel 0-19 is almost symmetrically opposite to 0-7 and both channels have similar time-averaged powers (6380 and 6369 kW). 0-19 was refulled at 57 FPD but the overpower at 60 FPD was only 1.5 percent.

The age and power history of the channels in the section of the core containing 0-7 were compared with the history of the channels neighbouring 0-19 on the other side of the core. These two sections

are defined in Fig. 40 and each contain 25 channels. The Local Average Age (LAA) and Local Average Power (LAP) about 0-7 and 0-19 have been calculated at 60 FPD and also at 50 and 40 FPD. These values and other relevant data are recorded in Table 17. Note that while the age and LAA at 60 FPD are similar, LAP $(0\text{-}7)_{60\ FPD}$ is considerably greater than LAP $(0\text{-}19)_{60\ FPD}$. This explains the high power at 0-7 at 60 FPD.

The reason for the high LAP $(0\text{-}7)_{60\ FPD}$ must now be decided. Relevant data are supplied in Table 18. The high value was caused by refuelling too many channels in the left half of the core in the energy interval 30 to 40 FPD.

A relatively large number of fresh bundles in the left half reach their plutonium peak 20 to 30 FPD after charging resulting in a large left to right power tilt. This reinforces the channel effect at 0-7 at 60 FPD.

During actual operation, the controllers would be filled differentially to remove the tilt and the high overpower at 0-7 would not occur. However, the fuelling engineer should attempt to keep the power distribution uniform to minimize stress on the control system.

4. SUMMARY AND CONCLUSIONS

Estimates of fuel management data for the equilibrium operation of a specific CANDU reactor, have been obtained using the code FMDP. Results are given in Table 15.

The collapsing procedure has been studied and improved. It was found that the use of time-averaged collapsed parameters in instantaneous calculations and simulations with coarse mesh gives a large saving in computing costs compared to fine mesh costs, with very little loss in accuracy.

Further testing needs to be done to determine the accuracy of calculations with instantaneous collapsed parameters. These would be used only in simulations when start conditions are known and can be regenerated periodically, after a fine mesh calculation with current reactor conditions, to maintain a desired level of accuracy.

The accuracy of coarse mesh calculations may be further increased by storing compound collapsed parameters. When these are used, the incremental cross-sections are dependent upon the cell conditions for the perturbation calculation.

5. REFERENCES

(1) D.M. Miller, "POWDERPUFS-V Users Manual, Part 2 of 3", TDAI-31, AECL Power Projects (Sept. 1973).

(2) A.L. Wight and R. Sibley, "Fuel Management Design Program Part 1 - Program Description", TDAI-105, AECL Power Projects (to be issued).

(3) A.L. Wight and R. Sibley, "Fuel Management Design Program Part 2 Users Guide and Programmers Manual", TDAI-106, AECL Power Projects (to be issued).

(4) A.L. Wight, "Fuel Management Studies for Bruce A Reactor", TDAI-77, AECL Power Projects.

(5) D.G. Parkinson, private communication.

(7) P.H. Stevens, "Power Peaking Analysis for the CANDU-PHW(PB) Study", PHW(PB)-N-15, CRNL (Dec. 1975).

(8) N.J. Abush, private communication.

TABLE 1 SUMMARY OF TIME-AVERAGED RESULTS FOR THE 8 BUNDLE SHIFT FUELLING SCHEME

VERSION OF FMDP	JUN1776TST	SEP0176ALW
Fission Power (kW)	2854600	2854600
Thermal Power (kW)	2695600	2695600
Max. Channel Power (kW)	6484	6480
Max. Bundle Power (kW)	796	799
Excess Reactivity with Zone Controllers at 40% Fill milli-k	0.40	0.42
Average Discharge Irradiation n/kb		
inner core	1.78	1.78
outer core	1.50	1.50
Zonal Power+		
Zone 1		364594
2		366415
3		416916
4		402966
5		413710
6		364594
7		366415

+ See Fig. 3 for Zonal Boundaries.

TABLE 2 RESULTS OF INSTANTANEOUS CALCULATION (NRAN=6389) WITH FINE MESH

VERSION OF FMDP	JUN1776TST	DEC0176ALW
Number of Mesh Points	13984	13984
Excess Reactivity milli-k	2.17	3.61
Max. Channel Power (kW) and Location	7999 D-11	8268 D-12
Max. Bundle Power (kW) and Location	1017 D-12, No.7	1037 D-12, No.7

TABLE 3 DEGREE OF PERTURBATION OF THE INSTANTANEOUS CALCULATION (NRAN=6389) WITH FINE MESH FROM THE TIME-AVERAGED CALCULATION

		CHANNEL POWER RATIOS	BUNDLE POWER RATIOS
Average	Whole Core	0.9963	0.9935
	Outer Region		
	Inner Region		
Std. Deviation		0.1331	0.1301
Maximum Ratio		1.25	1.289

TABLE 4 RESULTS OF INSTANTANEOUS CALCULATION (NRAN=6389) WITH VARIOUS COARSE MESH MODELS

CELL SIZE NUMBER OF MESH POINTS	1*1*1 7616	1*1*2 4352	1*1*4 2720	1*1*6 2176	2*2*2 1440
VERSION OF FMDP	JUN1776TST+	SEP0176ALW	DEC0176ALW	DEC0176ALW	DEC0176ALW
Excess Reactivity milli-k	2.22	3.61	3.56	3.42	3.44
Max. Channel Power (kW) and Location	8064 D-11	8270 D-12	8200 D-12	8081 D-12	8176 E-11
Max. Bundle Power (kW) and Location	1017 D-12,No.7	1038 D-12,No.7	1037 D-12,No.7	1008 D-12,No.7	1014 D-12,No.7
Channel Power at ‡ Location of Fine Mesh Maximum Value	8064	8270	8200	8081	8129
Percent Error	0.81	0.02	-0.82	-2.26	-1.68
Bundle Power at ‡ Location of Fine Mesh Maximum Value	1017	1038	1037	1008	1014
Percent Error	0.0	0.10	0.0	-2.30	-2.22

+ This version did not contain the CP Factor improvement.

‡ See Table 2.

TABLE 5 COMPARISON OF COARSE MESH INSTANTANEOUS RESULTS WITH THE FINE MESH ANSWER AS REFERENCE

		CHANNEL POWER RATIOS			BUNDLE POWER RATIOS			CELL FLUX RATIOS		
		AVERAGE	STD. DEV.	MAXIMUM	AVERAGE	STD. DEV.	MAXIMUM	AVERAGE	STD. DEV.	MAXIMUM
1*1*1 INSTAN / FINE MESH INSTAN	Whole Core	0.99985	0.01116	1.051	1.00893	0.03458	1.129	1.00883	0.03078	1.1154
	Outer	1.0008	0.00827	1.045						
	Inner	0.9987	0.01377	1.051						
1*1*2 INSTAN / FINE MESH INSTAN	Whole Core	1.000666	0.004461	1.020	1.000892	0.0049	1.0236	1.00045	0.0048	1.0236
	Outer	1.000799	0.004691	1.020						
	Inner	1.000506	0.004161	1.0091						
1*1*4 INSTAN / FINE MESH INSTAN	Whole Core	1.00211	0.0171	1.033	0.9925	0.01656	1.0612	0.99861	0.01649	1.0612
	Outer	1.0034	0.01328	1.033						
	Inner	1.000564	0.009261	1.0239						
1*1*6 INSTAN / FINE MESH INSTAN	Whole Core	1.005054	0.02989	1.0747	1.00254	0.0293	1.1058	1.001445	0.02845	1.1058
	Outer	1.006417	0.03446	1.0747						
	Inner	1.00342	0.02314	1.0614						
2*2*2 INSTAN / FINE MESH INSTAN	Whole Core	1.00269	0.0243	1.0666	1.00019	0.0240	1.0817	1.00145	0.0239	1.0817
	Outer	1.00447	0.02349	1.0666						
	Inner	0.9952	0.0243	1.0504						

TABLE 6 EXCESS REACTIVITY HISTORY

CELL SIZE NO. OF MESH POINTS ENERGY CLOCK FPD	1*1*1 14336	1*1*4 5120	1*1*6 4096	2*2*2 2592
5	0.014 milli-k	0.05	0.03	-0.103
10	-0.349	-0.259	-0.234	
20	-0.795	-0.697	-0.619	
25	-0.87	-0.762	-0.696	
30	0.08	0.11	0.08	
40	0.31	0.30	0.30	
50	-0.186	-0.147	-0.109	
60	0.18	0.18	0.22	
70	0.29	0.28	0.26	

TABLE 7 MAXIMUM CHANNEL POWER HISTORY

CELL SIZE / ENERGY CLOCK FPD	1*1*1	1*1*4	1*1*6	2*2*2
5	6918 kW at E-14	6870 D-14	6850 D-14	7046 D-14
10	6944 E-14	6896 E-14	6857 E-14	
20	7100 E-14	7049 E-14	6967 E-14	
25	6900 N-5	6868 N-5	6843 N-5	
30	7034 E-14	6986 E-14	6943 E-14	
40	6932 N-4	6897 N-4	6825 N-4	
50	6948 F-15	6912 F-15	6869 F-15	
60	7091 O-8	7039 O-8	6986 O-8	
70	6902 F-17	6881 N-4	6858 E-16	

TABLE 8 MAXIMUM BUNDLE POWER HISTORY

CELL SIZE / ENERGY CLOCK FPD	1*1*1	1*1*4	1*1*6	2*2*2
5	853 kW D-13,No.7	856 D-13,No.7	865 D-14,No.6	884 D-13,No.7
10	864 V-14,No.7	871 V-14,No.7	861 V-14,No.6	
20	867 Location not known+	867 D-15,No.7	858 D-13,No.7	
25	867 Location not known+	840 O-4,No.7	837 O-4,No.7	
30	862 D-15,No.7	866 D-15,No.7	854 D-15,No.7	
40	855 N-4,No.7	861 N-4,No.7	842 N-4,No.7	
50	826 D-11,No.7	829 D-11,No.7	828 D-11,No.7	
60	872 O-4,No.7	875 O-4,No.7	862 O-4,No.7	
70	860 N-4,No.7	868 N-4,No.7	852 N-4,No.7	

+ The bundle power data at this time step were lost.

TABLE 9 AVERAGE IRRADIATION OF DISCHARGED FUEL IN SELECTED BURNUP INTERVALS

CELL SIZE / BURNUP INTERVAL	AVERAGE IRRADIATION OF DISCHARGED FUEL IN BURNUP INTERVAL (n/kb)		
	1*1*1	1*1*4	1*1*6
5 to 10 FPD	Inner region = 1.770	1.770	1.770
	Outer region = 1.501	1.501	1.501
10 to 20 FPD	1.8107	1.8112	1.81145
	1.5108	1.5112	1.51146
50 to 60 FPD	1.7871	1.7886	1.7893
	1.5149	1.5163	1.5177
60 to 70 FPD	1.7427	1.7449	1.7454
	1.5024	1.5038	1.5052

TABLE 1C COMPARISON OF SIMULATION RESULTS WITH THE 1*1*1 ANSWER AS REFERENCE

ENERGY CLOCK FPD			CHANNEL POWER RATIOS 1*1*4/1*1*1	CHANNEL POWER RATIOS 1*1*6/1*1*1	BUNDLE POWER RATIOS 1*1*4/1*1*1	BUNDLE POWER RATIOS 1*1*6/1*1*1	CELL FLUX RATIOS 1*1*4/1*1*1	CELL FLUX RATIOS 1*1*6/1*1*1
5	AVERAGE	WHOLE CORE	0.99999	0.99996	0.99021	0.99038	0.99021	0.99038
		OUTER	0.999350	0.99880				
		INNER	1.000315	1.00156				
	STD.DEV	WHOLE CORE	0.002764	0.004649	0.0313	0.03677	0.031312	0.03677
		OUTER	0.00175	0.005468				
		INNER	0.002706	0.003491				
	MAX.	WHOLE CORE	1.00562	1.01159	1.0549	1.08665	1.0549	1.08665
		OUTER	1.00537	1.01086				
		INNER	1.00562	1.01159				
30	AVERAGE	W	1.000199	1.000367	0.99057	0.99074	0.99058	0.99076
		O	1.000509	1.000810				
		I	0.99979	0.99979				
	STD. DEV.	W	0.0032002	0.006191	0.03092	0.03148	0.03100	0.03158
		O	0.003440	0.006892				
		I	0.002805	0.005075				
	MAX.	W	1.007265	1.01459	1.05074	1.06446	1.05059	1.06592
		O	1.007265	1.01459				
		I	1.006553	1.01228				
60	AVERAGE	W	1.000343	1.000708	0.99157	0.9904	0.99158	0.99041
		O	1.001762	1.00343				
		I	0.998687	0.99715				
	STD.DEV	W	0.004025	0.008764	0.03048	0.03230	0.03065	0.03249
		O	0.003702	0.008562				
		I	0.003659	0.007682				
	MAX.	W	1.00983	1.02148	1.04638	1.0601	1.0464	1.06170
		O	1.00892	1.0203				
		I	1.00983	1.02148				
70	AVERAGE	W	1.000099	* ANALYZE NOT DONE FOR THIS CASE AT THIS BURNUP	0.99087		0.99089	
		O	0.996375					
		I	1.000702					
	STD.DEV	W	0.003758		0.03034		0.03056	
		O	0.003826					
		I	0.003578					
	MAX.	W	1.0090		1.04082		1.048	
		O	1.0090					
		I	1.00842					

ENERGY CLOCK FPD		BUNDLE IRRADIATION RATIOS 1*1*4/1*1*1	BUNDLE IRRADIATION RATIOS 1*1*6/1*1*1
5	AVERAGE	1.0000	1.0000
	STD. DEV.	0.0000	0.0000
	MAX	1.0000	1.0000
10	AVERAGE	0.99950	0.994423
	STD.DEV	0.00537	0.00654
	MAX	1.0512	1.0839
20	AVERAGE	0.99878	0.99865
	STD.DEV	0.00930	0.01097
	MAX	1.05032	1.08454
25	AVERAGE	0.99851	0.99836
	STD.DEV	0.01067	0.0124
	MAX	1.04812	1.08174
30	AVERAGE	0.99819	0.99796
	STD.DEV	0.01207	0.01341
	MAX	1.04774	1.0747
40	AVERAGE	0.99772	0.99750
	STD.DEV	0.01421	0.01497
	MAX	1.04729	1.06592
50	AVERAGE	0.99731	0.99711
	STD.DEV	0.01602	0.016741
	MAX	1.04732	1.06745
60	AVERAGE	0.99697	0.99667
	STD.DEV	0.01724	0.01795
	MAX	1.04589	1.0744
70	AVERAGE	0.99666	0.99631
	STD.DEV	0.01835	0.019068
	MAX.	1.04559	1.06238

TABLE III BREAKDOWN OF SYSTEM REQUIREMENTS FOR COLLAPSING PROCEDURE AND INSTANTANEOUS CALCULATION WITH HALF CORE GEOMETRIES

				FMDP COMPUTATION (FOR VERSION DEC0176)				
						INSTANTANEOUS CALCULATION		
CELL SIZE	NO. OF MESH POINTS	MAX. CM REQUIRED	MAX. ECS REQUIRED	GENERATION OF COARSE MESH CROSS SECTIONS IN PREPARATION FOR COLLAPSING	COLLAPSING PROCEDURE	READ DATA FROM MASS STORAGE GENERATE RANDOM DISTRIBUTION OF IRRADIATION COMPUTE CROSS SECTIONS FOR EACH MESH POINT	ITERATIVE FLUX CALCULATION 0.0776 m.ll.sec/iter / mesh point. 110 iterations	CALCULATION OF POWER DISTRIBUTION WRITE DATA TO MASS STORAGE
FINE MESH	13984	214000B	561363B WITH OVERFLOW TO SCRATCH FILE	———	———	175000B 64000 69 7.8 35.	132000B 46080 119.4 0 47.	14000B 51200 1.74 13 3.6
1*1*1	7616	NOT KNOWN	NOT KNOWN	154000B 55296 15. 4. 7.5	120000B 40960 14. 3. 5.8	140000B 49152 45 6.7 20.	127000B 44544 65 0. 25.	135000B 47616 1.5 10. 2.7
1*1*2	4352	150000B	253123B	144000B 51200 13.4 2. 6.0	104000B 34816 12. 3. 4.8	140000B 49152 23. 6. 10.	122000B 41984 37.1 0. 14.	135000B 47616 3. 4. 2.0
1*1*4	2720	150000B	170123B	136000B 48128 12.3 2. 5.4	74000B 30720 12. 3. 4.6	135000B 47616 21. 3.8 9.2	122000B 41984 23.2 0. 8.8	135000B 47616 1.5 2. 1.0
1*1*6	2176	150000B	153323B	134000B 47104 12.3 2. 5.4	72000B 29696 12. 3. 4.6	135000B 47616 20. 2.5 8.5	120000B 41984 18.6 0. 7.0	135000B 47616 2. 1.5 1.0
2*2*2	1440	150000B	67247B	132000B 46080 11.1 2. 4.8	66000B 27648 12. 3. 4.6	135000B 47616 20. 3.4 8.7	102000B 33792 12.3 0. 4.3	110000B 47616 1.5 2.0 1.0

KEY

MEAN CM	IN OCTAL
MEAN CM	IN DECIMAL
CP TIME	IN SECONDS
IO TIME	IN SECONDS
	COST IN $

READ DATA (~380 BLOCKS) FROM SEQUENTIAL FILE TO RANDOM-ACCESS MASS STORAGE	WRITE DATA (~380 BLOCKS) FROM MASS STORAGE TO TAPE
102000B 33792 40. 8. 9.3	102000B 33792 40 2 7.2

TABLE 12 BREAKDOWN OF SYSTEM REQUIREMENTS FOR COLLAPSING PROCEDURE AND SIMULATION WITH FULL CORE

CELL SIZE	NO. OF MESH POINTS	MAX. CM REQUIRED	MAX ECS REQUIRED	FMDP COMPUTATION (FOR VERSION DEC017G)					
				GENERATION OF COARSE MESH CROSS-SECTIONS IN PREPARATION FOR COLLAPSING	COLLAPSING PROCEDURE	SIMULATION TIME STEP			
						READ DATA FROM MASS STORAGE. BURN FOR 10 FPD WITH REFUELLING OF 27 CHANNELS	COMPUTE CROSS-SECTIONS FOR EACH MESH POINT AS FUNCTION OF IRRADIATION	ITERATIVE FLUX CALCULATION 0.0776 m.llsec/iter / mesh point 110 iterations	CALCULATION OF POWER DISTRIBUTION WRITE DATA TO MASS STORAGE FOR RESTART
FINE MESH	27360	>320000B	NOT KNOWN	—	—		270000B 94208 70. 9. 52.	250000B 86016 233.5 0. 144.	270000B 94208 1.7 30. 16.
1*1*1	14336	2660000B	567326B WITH OVERFLOW TO SCRATCH FILE	230000B 77824 28.3 15. 21.	140000B 49152 20. 10. 10.	226000B (WITH NO FRESH BUNDLES IN POOL) 76800 1.7 15 6.4	230000B 77824 50. 6. 31.	214000B 71680 122.4 0. 64.	236000B 80896 1.6 23. 8.
1*1*4	5120	2660000B	316000B	164000B 59392 30. 4. 16.	104000B 34816 15. 7. 6.5		164000B 59392 41. 4. 20.	150000B 53248 43.7 0. 19.	174000B 63488 1.3 4.5 2.
1*1*6	4096	2660000B	311326B	164000B 59392 28. 11. 16.	100000B 32768 15. 7. 6.3		164000B 59392 41. 4. 20.	150000B 53248 35.0 0. 15.	174000B 63488 1.3 3.8 1.7
2*2*2	2592	2660000B	143132B	155000B 55808 25.3 11. 14.	72000B 29696 15. 7. 6.2		155000B 55808 33. 3. 15.	112000B 37888 22.1 0. 10.	174000B 63488 1.3 4. 1.7

KEY

MEAN CM IN OCTAL
MEAN CM IN DECIMAL
CP TIME IN SECONDS
IO TIME IN SECONDS
COST IN $

READ DATA FROM SEQUENTIAL FILE TO MASS STORAGE (~ 850 BLOCKS)	WRITE DATA FROM MASS STORAGE TO SEQUENTIAL FILE (~ 850 BLOCKS)
1020000B 33792 80. 20. 20.	1020000B 33792 80. 4. 14.

TABLE 13 COMPARISON OF COMPUTING COSTS

ELL SIZE (1/2 Core)	COMPUTING COSTS+ $	
	TOTAL FOR 1 READ TAPE 1 COLLAPSING PROCEDURE 1 INSTANTANEOUS CALC. 1 RITE TAPE	TOTAL FOR 10 READ TAPES 1 COLLAPSING PROCEDURE 10 INSTANTANEOUS CALCS. 10 RITE TAPES
FINE MESH	102	1020
1*1*1	77.5	655
1*1*2	53.3	436
1*1*4	45.5	365
1*1*6	43.0	340
2*2*2	39.9	314
ELL SIZE (FULL CORE)	TOTAL FOR 1 READ TAPE 1 COLLAPSING PROCEDURE 1 SIMULATION TIME STEP (10 FPD WITH REFUELLING) 1 WRITE TO TAPE	TOTAL FOR 1 READ TAPE 1 COLLAPSING PROCEDURE 10 SIMULATION TIME STEPS 1 WRITE TO TAPE
FINE MESH	252	2214
1*1*1	166	1075
1*1*4	104	531
1*1*6	99	483
2*2*2	81	322

+ Calculated from TABLES 11 and 12.

TABLE 14 MAXIMUM CHANNEL AND BUNDLE POWERS OBTAINED DURING SIMULATION

ENERGY CLOCK FPD	MAXIMUM CHANNEL POWER (kW) AND LOCATION	MAXIMUM BUNDLE POWER (kW) AND LOCATION	MAXIMUM CHANNEL OVERPOWER (%) AND LOCATION
0	6865 M-5	832	8.48 M-1
5	6918 E-14	853 D-13,No.7	9.10 E-14
10	6944 E-14	864 V-14,No.7	9.50 E-14
20	7100 E-14	867 LOCATION NOT KNOWN+	12.5 A-14
25	6900 N-5	867 LOCATION NOT KNOWN+	9.50 N-1
30	7034 E-14	862 D-15,No.7	10.92 E-14
40	6932 N-4	855 N-4,No. 7	6.57 N-1
50	6948 F-15	826 D-11,No.7	11.00 E-22
60	7091 O-8	872 O-4,No. 7	10.75 O-7
70	6902 F-17	860 N-4,No. 7	9.40 A-16

+ The bundle power data at this time step were lost.

TABLE 15 SUMMARY OF EQUILIBRIUM FUEL MANAGEMENT DATA OBTAINED WITH NORMAL MESH MODEL

Fission Power (kW)		2854600
Thermal Power (kW)		2695600
Maximum Channel Power (kW)		7100
Maximum Bundle Power (kW)		874
Average Maximum Channel Power (kW)		6963
Average Maximum Bundle Power (kW)		856
Feed Rate (Bundles/Day)	Whole Core	22.569
	Inner Region	10.237
	Outer Region	12.332
Average Exit Irradiation	Whole Core	1.628
	Inner Region	1.775
	Outer Region	1.506

TABLE 16 POWER TILT AND FUELLING HISTORY

ENERGY CLOCK FPD	0		5		10		20		25		30		40		50		60		70
	ZONAL † OVERPOWER	NO. OF CHANNELS FUELLED IN NEXT ENERGY INTERVAL																	
ZONE 1	1.028	0	0.983	2	0.972	2	1.001	3	1.016	2	0.972	5	1.015	3	1.005	4	1.036	4	1.022
2	1.027	1	0.990	1	0.983	4	0.963	3	1.035	2	0.957	5	1.019	3	0.951	4	1.041	4	0.989
3	0.972	4	1.022	2	1.037	3	1.060	0	0.956	5	1.036	1	0.973	7	1.043	4	0.984	5	1.030
4	1.001	0	0.977	2	0.994	4	0.993	2	0.995	3	1.001	5	1.024	3	1.011	5	1.035	2	0.984
5	0.944	2	1.017	3	1.038	3	0.962	1	1.024	4	1.008	4	0.991	4	0.956	4	0.986	3	0.936
6	0.984	0	0.997	1	0.976	4	1.046	2	0.974	2	1.020	4	0.998	5	1.050	2	0.956	5	1.037
7	0.999	1	1.012	0	0.989	4	0.972	3	1.004	2	0.997	4	0.982	5	0.985	5	0.961	6	1.007
OVERALL POWER TILT AND FUELLING HISTORY		NO. OF CHANNELS FUELLED IN NEXT ENERGY INTERVAL																	
$100 \times \frac{\Sigma P_{TOP} - \Sigma P_{BOTTOM}}{\Sigma P_{TOTAL}}$	-0.68%	TOP 4	-0.327	6	-0.458	12	3.23	5	-1.95	11	0.996	12	-0.275	17	3.20	12	-0.292	17	2.63
		BOTTOM 4		5		12		10		9		16		13		16		13	
$100 \times \frac{\Sigma P_{LEFT} - \Sigma P_{RIGHT}}{\Sigma P}$	1.355%	LEFT 2	-0.904	5	-0.683	13	-1.225	9	1.24	9	-2.1	17	0.91	12	-1.64	14	2.64	14	-0.687
		RIGHT 6		6		11		6		11		11		18		14		16	

† ZONAL OVERPOWER $= \frac{\Sigma P_{\text{ZONE } i}}{\text{TIME-AVERAGED } \Sigma P_{\text{ZONE } i}}$

TABLE 17 COMPARISON OF CORE CONDITIONS ABOUT CHANNELS 0-7 AND 0-19 IN BURNUP INTERVAL 40 → 60 FPD

ENERGY CLOCK FPD	CHANNEL 0-7				CHANNEL 0-19			
	AGE	POWER kW	LAA^{+}_{8CHNLS}	$LAP^{\ddagger}_{8CHNLS}$ kW	AGE	POWER kW	LAA_{8CHNLS}	LAP_{8CHNLS} kW
40	0.925	6295	0.535	6698	0.918	6151	0.531	6530
50	0.965	5858	0.578	6280	0.958	6022	0.564	6441
60	0.343	7071	0.618	6883	0.336	6462	0.607	6282

+ LAA_{8CHNLS} (0-7) is the average age of the 8 channels next to 0-7 (see Reference 5)

‡ LAP_{8CHNLS} (0-7) is the average power of the 8 channels next to 0-7

TABLE 18 LEFT TO RIGHT POWER TILT AND FUELLING HISTORY IN BURNUP INTERVAL 30 → 60 FPD

ENERGY CLOCK FPD	LEFT TO RIGHT POWER TILT PERCENT	NUMBER OF CHANNELS FUELLED IN NEXT BURNUP INTERVAL
30	-2.1	Left 17 Right 11
40	0.91	Left 12 Right 18
50	-1.64	Left 14 Right 14
60	2.64	

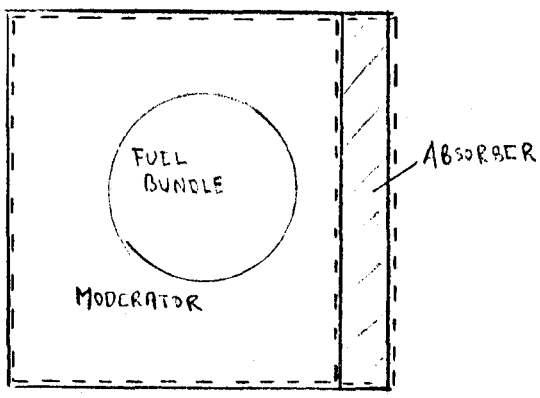

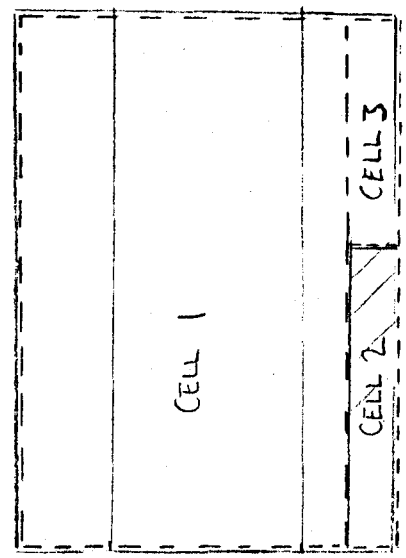

---- FINE MESH CELL BOUNDARIES

FIG. 1a FINE MESH CELL BOUNDARIES

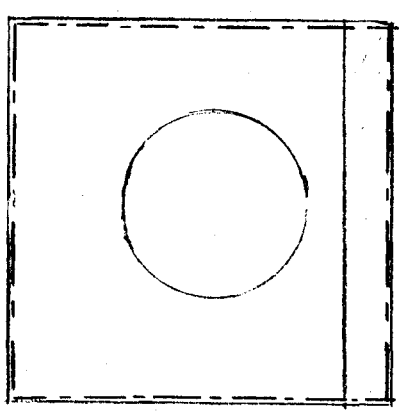

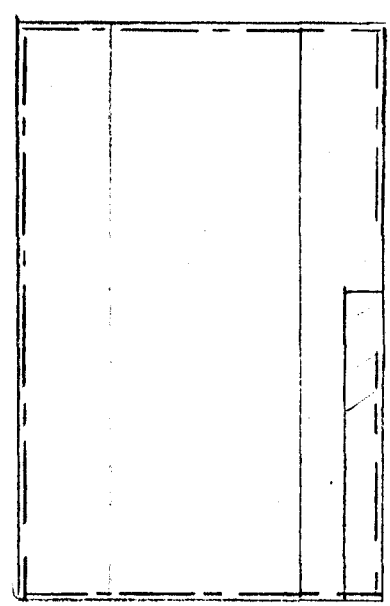

— · — · — NORMAL MESH CELL BOUNDARIES

FIG. 1b NORMAL MESH CELL BOUNDARIES

X-DIRECTION

	1	2	3	4	5	6	7	8	9	10	11	12
0.0	22.85	28.575	28.575	28.575	28.575	28.575	28.575	28.575	24.13	8.89	9.843	28.575

13	14	15	16	17	18	19	20	21	22	23
9.843	8.89	24.13	24.13	8.89	24.13	24.13	8.89	9.843	14.288	0.0

Y-DIRECTION

1	2			31	32
0.0	22.85	←	28 x 28.575 →	22.85	0.0

Z-DIRECTION

1	2	3	4	5	6	7	8	9	10	11	12
0.0	47.625	50.8	49.53	49.53	15.24	8.89	35.56	35.56	8.89	35.56	35.56

13	14	15	16	17	18	19
8.89	15.24	49.53	49.53	50.8	47.625	0.0

FIG. 2 HALF CORE FINE MESH SPACINGS (REF. 4)

DATE 23/11/7- TIME 22.02.3- CURRENT MEMORY PARTITION USED USER NAME = C.OLIVE EY551

*PRINT RUN TIME 223.576 I/O TIME 138.178

CHANNEL POWERS IN KILOWATTS

TOTAL REACTOR POWER IS 2695.00 MEGAWATTS
TOTAL FISSION POWER IS 2654.00 MEGAWATTS
MAXIMUM CHANNEL POWER IS 6479.9- KILOWATTS
MAXIMUM BUNDLE POWER IS 795.76 KILOWATTS

	1	2	3	4	5	6	7	8	9	10	11	12
A								3422	5695	5994	4181	4219
B						3432	5792	4374	4792	5072	5240	5257
C					3811	4256	4720	5330	5704	5940	6066	6057
D				3718	4599	5071	5491	5999	6268	6418	6480	6428
E			3610	4392	5113	5663	5986	6351	6379	6431	6342	6223
F		3258	4195	5025	5628	5970	6082	6318	6300	6298	6246	6033
G		3853	4775	5516	5930	6068	6019	6221	6265	6262	6179	5949
H		4396	5260	5858	6028	5979	5970	6199	6269	6260	6181	5948
J	3723	4700	5614	6116	6050	5925	5951	6210	6276	6284	6214	6006
K	3984	5044	5888	6298	6173	5983	6005	6239	6313	6317	6282	6143
L	4199	5257	6055	6357	6272	6102	6099	6309	6350	6358	6323	6206
M	4310	5352	6151	6422	6376	6264	6269	6371	6390	6370	6330	6200
N	4311	5368	6162	6463	6419	6356	6348	6431	6413	6385	6313	6143
O	4219	5279	6110	6430	6428	6369	6380	6449	6437	6391	6306	6083
P	3996	5080	5940	6407	6344	6323	6353	6432	6420	6392	6310	6100
Q	3734	4755	5660	6187	6202	6196	6238	6360	6387	6375	6335	6198
R		4413	5278	5908	6091	6104	6089	6292	6347	6379	6352	6248
S		3867	4797	5522	5924	5995	5983	6227	6324	6359	6358	6253
T		3269	4129	5012	5540	5773	5888	6254	6298	6339	6327	6211
U			3589	4346	5001	5438	5750	6212	6311	6374	6276	6104
V				3460	4314	4941	5343	5886	6162	6341	6308	6149
W					3565	4225	4884	5245	5600	5803	5873	5765
X						3431	3781	4319	4703	4957	5093	5106
Y								3381	3632	3909	4048	4143

1 2 3 4 5

——— REGION BOUNDARY
— — — ZONE BOUNDARY

FIG. 3 TIME-AVERAGED CHANNEL POWER DISTRIBUTION

CHANNEL	BUNDLE NO. 1	2	3	4	5	6	7	8	9	10	11	12	13
D-12	65.0	255.5	458.7	599.9	685.1	778.9	796.8	779.7	682.4	586.3	436.8	241.2	61.8
M-11	70.6	264.8	463.3	602.5	641.7	707.9	708.3	710.5	652.2	633.7	505.8	292.3	76.0
Q-1	25.7	116.9	232.2	339.0	412.0	467.5	479.3	472.2	425.1	357.6	251.1	127.7	28.0
E-11	68.7	268.0	474.4	616.2	664.0	747.2	750.5	750.1	661.2	594.4	439.7	243.9	63.5
N-12	71.2	265.6	457.8	571.8	604.2	698.6	698.2	699.5	611.2	599.0	498.5	291.4	76.0
L-1	34.1	145.6	278.4	390.3	462.2	521.8	538.4	529.6	471.1	390.3	268.6	137.2	32.0
A-11	34.5	146.8	279.9	389.9	461.7	523.7	537.1	524.8	460.9	382.8	267.8	138.6	32.5
T-2	19.3	97.6	202.3	297.8	361.7	412.7	425.2	417.6	372.7	313.9	219.5	107.2	21.2

FIG. 4 REFERENCE (TIME-AVERAGED) BUNDLE POWERS FOR 8 SPECIFIC CHANNELS

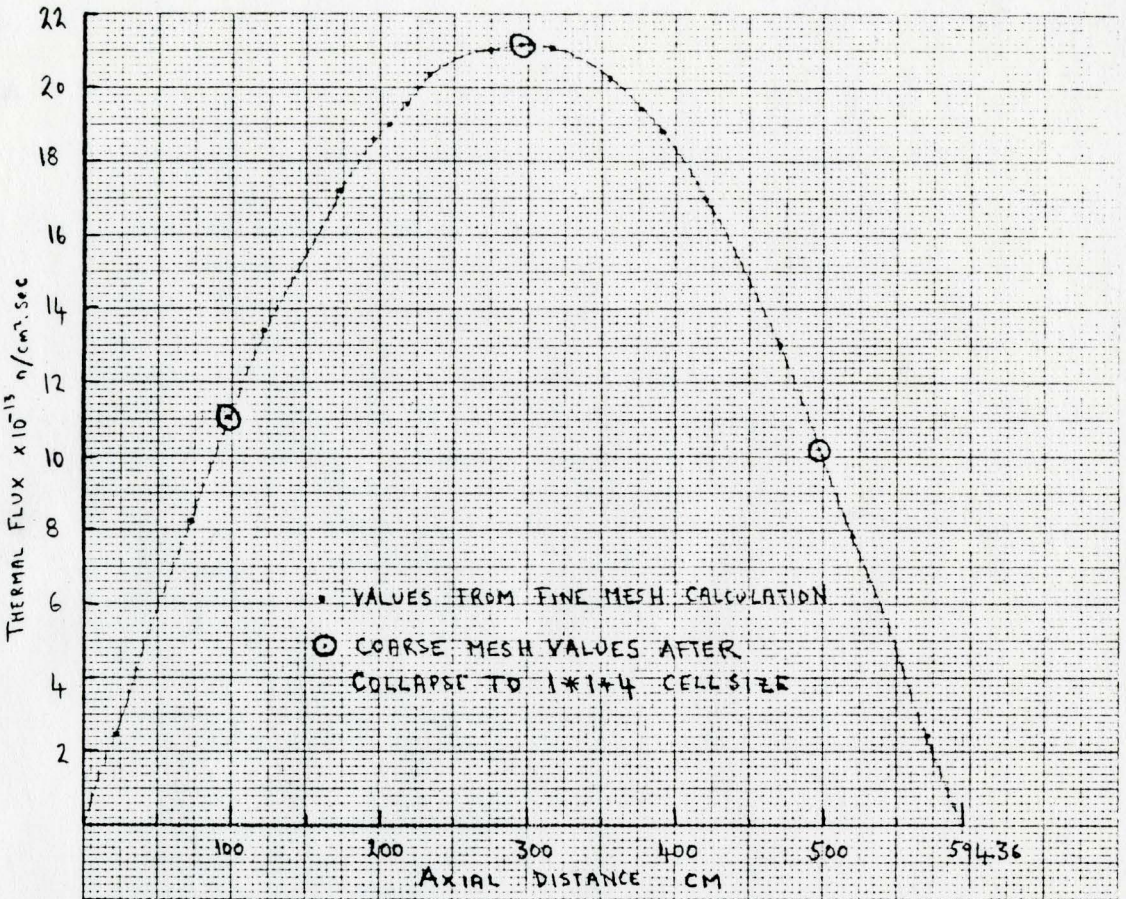

FIG. 5a REFERENCE THERMAL FLUX DISTRIBUTION ALONG CHANNEL D-4

12.57	55.95	109.12	153.69	182.52	205.88	211.01	205.74	180.73	150.29	104.96	53.18	11.69

$\times 10^{-10}$ n/cm².sec

FIG. 5b CELL FLUX DISTRIBUTION ALONG D-4 WHICH RESULTS AFTER VOLUME WEIGHT AVERAGING THE FINE MESH DISTRIBUTION OVER THE LATTICE CELL ARRAY

25.40	110.80	110.80	110.80	154.85	198.90	198.90	198.90	150.40	101.90	101.90	101.90	50.95

$\times 10^{-10}$ n/cm².sec

FIG. 5c CELL FLUX DISTRIBUTION ALONG D-4 WHICH RESULTS AFTER VOLUME WEIGHT AVERAGING THE COARSE MESH DISTRIBUTION OVER THE LATTICE CELL ARRAY

0.223	0.505	0.985	1.387	1.179	1.035	1.061	1.034	1.200	1.475	1.027	0.523	0.229

FIG. 5d CP FACTOR DISTRIBUTION FOR CHANNEL D-4

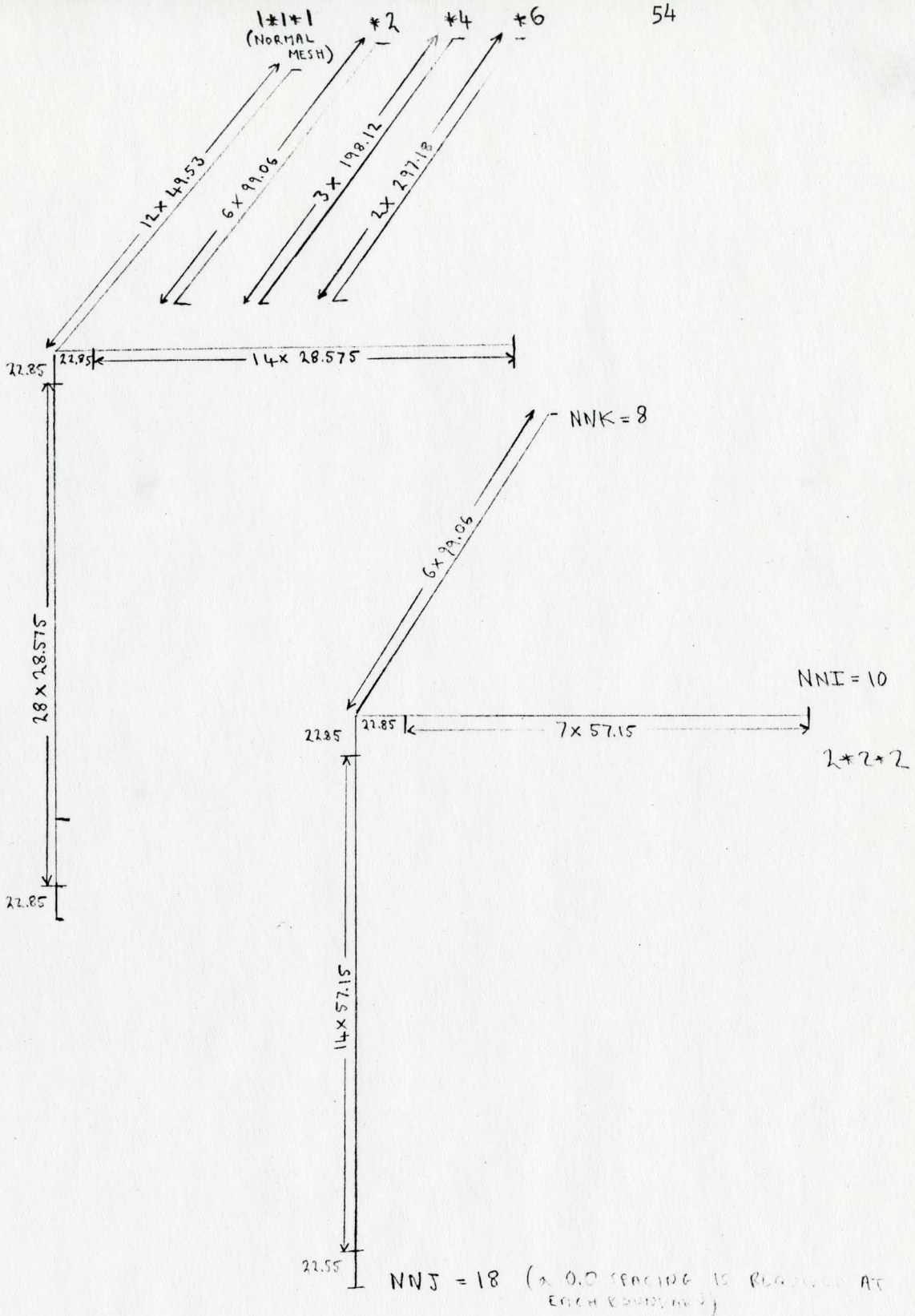

FIG. 6 HALF CORE COARSE MESH SPACINGS

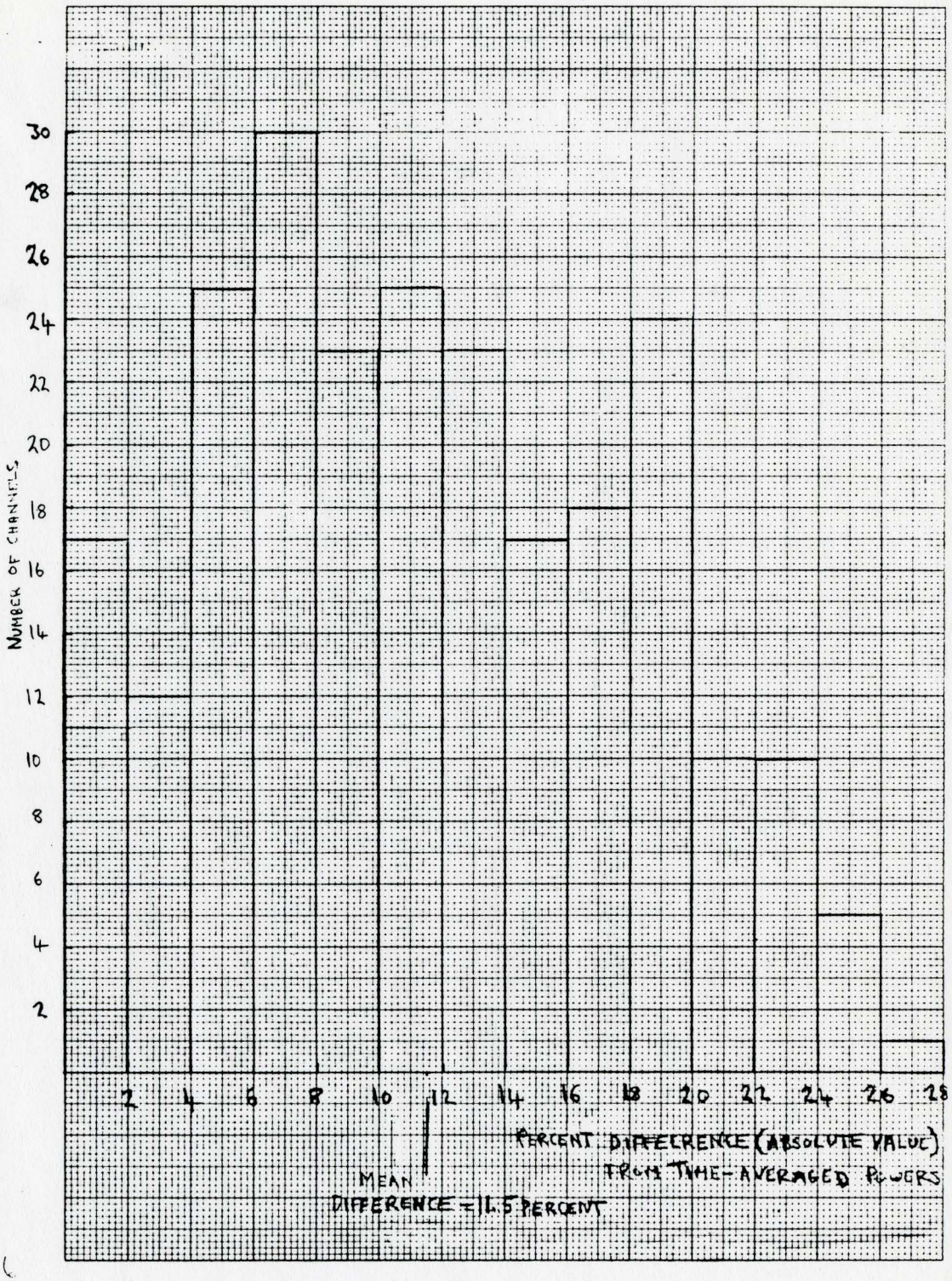

FIG. 7 COMPARISON OF THE CHANNEL POWERS OBTAINED FROM THE FINE MESH INSTANTANEOUS CALCULATION (NRAN=6389) WITH THE TIME-AVERAGED VALUES

		BUNDLE NUMBER												
		1	2	3	4	5	6	7	8	9	10	11	12	13
FINE MESH	ΣP ↓ 8268	80.6	318.8	582.0	768.8	883.5	1012.6	1037.5	1012.4	878.5	751.7	557.5	305.3	77.5
1*1*6 WITHOUT CP FACTORS	7796	322.9 300	650.3 104	657.1 12.9	659.3 -14.2	659.0 -25.4	657.7 -35.0	657.4 -36.6	657.8 -35.0	656.6 -25.3	646.0 -14.1	632.7 13.5	626.5 105	312.7 303
1*1*6 WITH CP FACTORS	8082	80.4 -0.25	315.3 -1.10	571.0 -1.89	752.1 -2.30	861.6 -2.48	982.2 -3.00	1007.5 -2.89	987.7 -2.44	861.4 -1.95	737.0 -1.955	547.0 -1.88	301.2 -1.34	76.9 -0.77

CHANNEL D-12

KEY

BUNDLE POWER PERCENT ERROR

FIG. 8 EFFECT OF THE CP FACTORS ON THE ACCURACY OF THE 1*1*6 INSTANTANEOUS CALCULATION WITH NRAN=6389

	BUNDLE NUMBER	1	2	3	4	5	6	7	8	9	10	11	12	13
FINE MESH	ΣP ↓ 7997	75.6	300.4	554.1	743.1	861.3	992.0	1017.1	991.8	854.8	722.6	527.2	285.1	71.9
1*1*1	8052	81.2	298.7	557.7	748.4	884.4	983.7	1017.1	983.0	878.2	727.6	530.6	283.5	77.4
	0.69	7.41	-0.57	0.65	0.71	2.68	-0.84	0.0	-0.89	2.74	0.69	0.64	-0.56	7.65

CHANNEL D-12

FINE MESH	5803	67.4	248.0	425.9	546.2	584.1	640.3	638.7	640.3	596.5	584.4	476.1	282.0	73.4
1*1*1	5797	71.7	244.7	424.9	544.9	599.5	621.0	640.7	621.7	612.0	583.3	475.4	278.5	78.2
	-0.10	6.38	-1.33	-0.23	-0.24	2.64	-3.01	0.31	-2.90	2.30	-0.19	-0.15	-1.24	6.54

CHANNEL M-11

FINE MESH	3285	24.0	107.6	209.8	301.8	364.7	406.6	412.0	403.7	367.1	314.8	228.0	118.9	26.1
1*1*1	3270	26.1	105.4	208.4	299.7	367.9	400.3	408.0	398.3	370.6	313.4	227.1	116.9	28.3
	-0.46	8.75	-2.04	-0.67	-0.69	0.88	-1.55	-0.98	-1.34	0.95	-0.44	-0.39	-1.68	8.43

CHANNEL Q-1

FIG. 9 COMPARISON OF BUNDLE POWERS GENERATED BY THE INSTANTANEOUS CALCULATION (NRAN=6389) WITH FINE MESH AND NORMAL MESH MODEL WITHOUT CP FACTORS

CHANNEL D-12

BUNDLE NUMBER → / ΣP ↓	1	2	3	4	5	6	7	8	9	10	11	12	13
FINE MESH 8268	80.6	318.8	582.0	769.8	883.5	1012.6	1037.5	1012.4	878.5	751.7	557.5	305.3	77.5
1+1+2 8270 0.02	80.9 0.37	320.6 0.56	582.2 0.03	769.6 -0.02	883.1 -0.05	1010.3 -0.23	1038.0 0.05	1010.8 -0.16	878.2 -0.03	752.2 0.07	559.0 0.27	307.3 0.65	78.1 0.77
1+1+4 8200 -0.82	80.3 -0.37	314.9 -1.32	570.2 -2.0	751.1 -2.4	878.7 -.55	1013.1 0.05	1036.9 -0.06	1014.1 0.17	876.7 -0.2	738.0 -1.82	547.9 -1.72	301.6 -1.2	77.0 -0.64
1+1+6 8082 -2.27	80.4 -0.25	315.3 -1.10	571.0 -1.89	752.1 -2.30	861.6 -2.48	982.2 -3.04	1007.5 -2.89	987.7 -2.44	861.4 -1.95	737.0 -1.955	547.0 -1.88	301.2 -1.34	76.9 -0.77
2+2+2 8129 -1.68	81.0 0.5	317.6 -0.38	574.0 -1.37	755.5 -1.85	867.7 -1.79	991.2 -2.1	1014.6 -2.2	992.4 1.97	865.2 -1.5	740.0 -1.56	549.6 -1.41	302.7 -0.85	77.3 -0.26

CHANNEL M-11

	1	2	3	4	5	6	7	8	9	10	11	12	13
6413	75.2	277.2	475.1	604.9	641.7	701.1	698.7	701.4	656.4	648.9	533.2	316.8	82.4
6381 -0.5	75.1 -0.13	276.2 -0.36	475.2 0.01	601.1 -0.63	636.2 -0.85	698.0 -0.46	694.7 -0.67	699.2 -0.31	650.4 -0.91	644.3 -0.71	533.3 0.02	315.3 -0.47	82.2 -0.24
6381 -0.5	73.7 -2.0	272.0 -1.87	468.7 -1.35	604.0 -0.15	638.8 -0.45	698.6 -0.06	698.9 0.03	701.0 -0.06	656.2 -0.03	651.3 0.37	527.3 -1.1	310.7 -1.92	80.6 -2.18
6427 0.22	73.6 0.22	270.8 -2.3	466.7 -1.77	601.4 -0.58	646.3 0.72	714.4 1.90	715.4 2.39	718.1 2.38	663.5 1.082	645.9 -0.46	522.9 -1.93	308.2 -2.71	79.9 -3.03
6572 2.45	78.0 3.7	288.0 3.9	484.2 1.9	616.8 1.97	653.9 1.9	713.8 1.81	714.8 2.3	717.7 2.32	674.6 2.77	669.1 3.11	546.3 2.46	328.0 3.5	85.1 3.28

CHANNEL Q-1

BUNDLE NUMBER → / ΣP ↓	1	2	3	4	5	6	7	8	9	10	11	12	13
FINE MESH 3090	22.7	101.4	197.5	283.8	342.6	381.7	386.9	379.4	345.5	296.7	215.2	112.4	24.7
1+1+2 3091 0.03	22.6 -0.44	100.9 -0.47	198.0 0.25	283.6 -0.07	342.3 -0.09	382.4 0.18	387.2 0.08	380.4 0.26	345.1 -0.09	296.6 0.03	215.7 0.23	111.9 -0.44	24.6 -0.40
1+1+4 3114 0.78	22.3 -1.76	100.1 -0.79	196.4 -0.56	284.6 0.28	341.4 -0.35	382.6 0.23	391.4 1.16	386.1 1.76	352.5 1.03	303.4 2.26	216.9 0.79	111.8 -0.53	24.3 -1.6
1+1+6 3137 1.49	22.3 -1.76	100.2 -1.18	196.7 -0.41	285.0 0.42	347.2 1.34	392.1 2.72	397.9 2.84	389.6 1.98	353.7 2.37	301.3 1.55	215.4 0.093	111.1 -1.16	24.1 -2.43
2+2+2 3125 1.13	22.6 -0.44	101.6 0.20	196.2 -0.61	282.6 -0.42	342.3 -0.09	385.0 0.86	393.3 1.65	387.5 2.13	354.0 2.46	303.8 2.39	218.0 1.3	113.4 0.89	24.7 0.0

FIG. 10 COMPARISON OF BUNDLE POWERS GENERATED BY THE INSTANTANEOUS CALCULATION (NRAN = 6389) WITH FINE MESH AND VARIOUS COARSE MESH GEOMETRIES

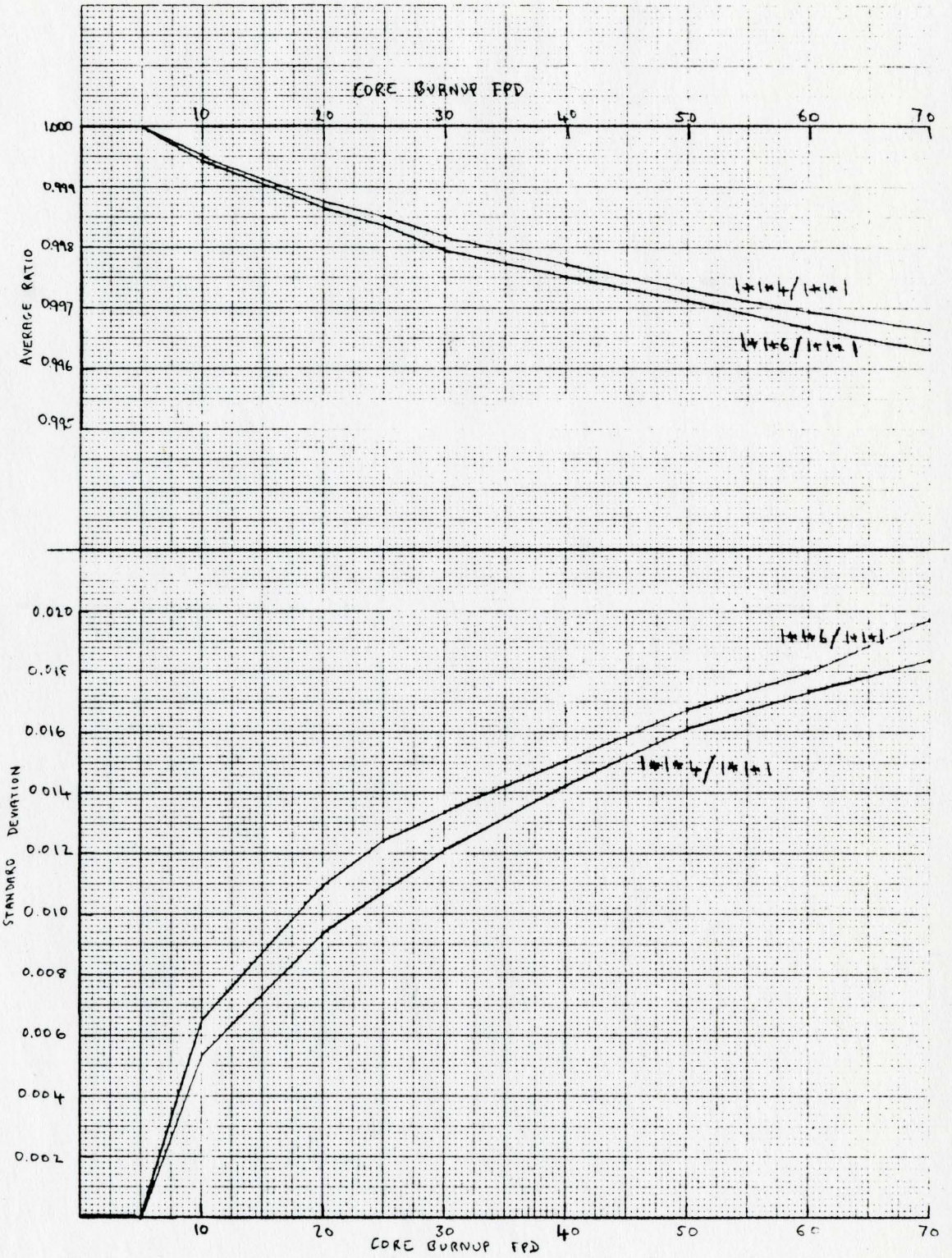

FIG. 11 COMPARISON OF IRRADIATION DISTRIBUTIONS WITH CASE 1*1*1 AS REFERENCE

BUNDLE NUMBER →		1	2	3	4	5	6	7	8	9	10	11	12	13
	↓ΣP													
1*1*1	6918	75.6	275.0	511.4	690.4	759.6	799.5	824.2	789.7	731.5	644.3	481.8	262.9	72.5
1*1*4	6861	71.9	280	509.5	683.3	727.3	815.6	819.2	818.6	705.1	624.2	473.2	264.7	68.2
	-.92	-4.9	1.8	-.37	-1	-4.2	2.9	-0.6	3.4	-3.6	-3.1	-1.7	0.68	-5.9
1*1*6	6833	73.3	285.4	519.3	696.5	763.9	836.0	804.6	768.8	677.2	623.1	472.4	264.2	68.1
	-1.23	-3	3.78	1.54	0.9	-2.1	4.6	-2.4	-2.6	-7.4	-3.3	-1.9	0.8	-6.1
2*2*2	6939	71.1	277	510.6	688.7	734.5	824.4	823.7	818.7	714.3	649.6	488.7	268.6	69.2
	0.3	-5.9	0.72	-.2	-2.5	-3.3	3.1	-0.1	3.7	-2.4	0.82	1.4	2.2	-4.5

FIG. 12 COMPARISON OF BUNDLE POWERS ALONG CHANNEL E-14 AT 5FPD

	1	2	3	4	5	6	7	8	9	10	11	12	13
6680	74.1	262.5	473.7	631.3	718.0	767.9	796.7	767.7	718.2	641.9	488.8	267.9	73.9
6665	69.2	265.2	475.3	637.8	698.6	786.9	790.1	789.6	695.4	636.4	488.8	268.1	68.4
-.22	-6.6	1	0.34	1.03	-2.7	2.5	-0.5	2.8	-3.2	-0.86	-1.02	0.1	7.4
6681	68.6	262.7	470.9	631.8	701.3	796.3	794.1	788.0	696.7	642.3	488.3	270.6	69.0
0.01	-7.4	1.02	-0.59	0.09	-2.3	3.7	-0.97	2.64	3.0	0.96	-.1	1.01	6.6

FIG. 13 COMPARISON OF BUNDLE POWERS ALONG CHANNEL E-14 AT 70FPD

ENERGY CLOCK FPD →	5	10	20	25	30	40	50	60	70
1*1*1	6918	6944	7100	6299	7034	6417	6902	6320	6680
1*1*4	6861	6896	7049	6329	6987	6435	6878	6351	6665
	-0.92	-0.89	-0.72	0.48	-0.67	0.28	-.35	0.47	-0.22
1*1*6	6833	6857	6967	6353	6943	6456	6846	6376	6681
	-1.23	-1.25	-1.87	0.86	-1.3	0.61	-0.8	0.89	0.01
2*2*2	6939								
	0.30								

FIG. 14 COMPARISON OF CHANNEL E-14 POWERS THROUGHOUT SIMULATION

5	10	20	25	30	40	50	60	70
0.363	0.401	0.476	0.514	0.548	0.623	0.69	0.762	0.828
0.363	0.400	0.475	0.513	0.547	0.621	0.689	0.761	0.827
0.363	0.400	0.475	0.512	0.546	0.620	0.688	0.759	0.826
0.363								

FIG. 15 COMPARISON OF CHANNEL E-14 AVERAGE BUNDLE IRRADIATION THROUGHOUT SIMULATION

BUNDLE NUMBER → / ZP ↓	1	2	3	4	5	6	7	8	9	10	11	12	13
1+1+1 6169	79.9	283.1	496.9	600.2	634.7	679.2	703.3	672.8	631.1	585.6	466.0	263.5	74.9
1+1+4 6177 0.13	75.7 -5.3	288.6 1.94	498.9 0.81	605.7 0.92	617.7 -3.47	703.6 3.6	703.1 -0.03	704.3 4.68	610.3 -3.29	578.0 -1.30	462.0 -0.86	264.7 0.46	70.0 6.54
1+1+6 6179	76.7 -4	292.4 3.28	505.5 2.14	613.8 2.26	629.1 -0.88	728.6 7.27	701.2 -0.298	675.7 0.43	593.0 -6.04	572.9 -2.17	458.0 -1.72	262.4 -0.62	69.4 -7.34
2+2+2 6096	74.3 -7.01	283.5 0.14	486.9 -1.62	589.3 -1.82	602.2 -5.12	695.6 2.41	692.1 -1.59	690.3 1.60	603.1 -4.46	579.7 -1.01	463.3 -0.58	265.5 1.76	70.2 -6.27

FIG. 16 COMPARISON OF BUNDLE POWERS ALONG CHANNEL N-13 AT 5FPD

	1	2	3	4	5	6	7	8	9	10	11	12	13
6043	78.8	281.7	488.6	587.2	621.0	664.8	691.1	665.5	616.4	562.0	451.1	260.0	75.3
1+1+4 6059 0.26	74.3 -5.71	287.3 1.99	494.8 1.27	596.5 1.58	604.4 2.47	689.8 3.76	689.2 -0.27	690.6 3.71	595.2 -3.44	558.4 0.648	447.9 -0.71	260.7 0.27	70.1 -6.91
1+1+6 6071 0.46	73.8 -6.34	285.2 1.24	491.2 0.53	592.2 0.85	606.2 2.38	696.4 4.75	692.4 0.19	690.3 3.73	596.8 -3.18	562.5 0.09	451.2 0.02	262.7 1.04	70.6 -6.24

FIG. 17 COMPARISON OF BUNDLE POWERS ALONG CHANNEL N-13 AT 70FPD

ENERGY CLOCK → / FPD ↓	5	10	20	25	30	40	50	60	70
1+1+1	6169	6415	6286	6352	6338	6517	6327	6647	6043
1+1+4	6177 0.13	6400 -0.23	6287 0.02	6348 -0.06	6328 -0.16	6491 -0.40	6319 -0.13	6427 -0.31	6059 0.26
1+1+6	6179 0.16	6387 -0.46	6277 -0.14	6334 -0.28	6322 -0.25	6475 -0.64	6313 -0.22	6409 -0.59	6071 0.46
2+2+2	6096 1.19								

FIG. 18 COMPARISON OF N-13 CHANNEL POWERS THROUGHOUT SIMULATION

5	10	20	25	30	40	50	60	70
0.519	0.552	0.620	0.654	0.687	0.753	0.821	0.887	0.954
0.519	0.552	0.620	0,653	0.687	0.753	0.821	0.887	0.953
0.519	0.552	0.620	0.653	0.687	0.753	0.820	0.886	0.953
0.519								

FIG. 19 COMPARISON OF N-13 CHANNEL AVERAGE BUNDLE IRRADIATION THROUGHOUT SIMULATION

BUNDLE NUMBER → 1	2	3	4	5	6	7	8	9	10	11	12	13
1+1+1 Σp ↓ 4082	37.2	146.1	282.6	392.3	465.9	504.3	515.2	499.9	453.2	367.1	254.5	129.9	33.4
1+1+4 4082 0.0	34.4 7.5	147.5 0.7	281.8 -0.28	392.3 0.0	453.7 -2.62	504.6 0.06	519.7 0.87	511.5 2.32	452.0 -.265	367.9 0.22	254.5 0.0	131.1 0.92	30.7 8.1
1+1+6 4101 0.46	34.8 -6.5	149.6 2.4	285.7 1.1	397.9 1.43	468.3 0.51	525.6 4.22	523.0 1.51	496.9 -0.6	442.0 -7.5	364.6 -0.68	252.2 -0.90	129.9 0.0	30.5 -8.7
2+2+2 4076 -0.15	33.9 -8.4	145.6 -0.24	278.7 1.58	388.3 -1.82	454.4 -2.5	508 0.73	520.7 1.1	510.1 2.04	450.8 -0.53	368.7 0.43	254.8 0.12	130.9 0.77	30.7 -8.1

FIG. 20 COMPARISON OF BUNDLE POWERS ALONG CHANNEL L-1 AT 5FPD

	1	2	3	4	5	6	7	8	9	10	11	12	13
4433	38.2	148.5	288.9	409.9	497.5	549.0	566.0	550.1	500.9	417.9	287.5	142.9	35.8
4421 -0.27	35.6 -6.8	150.5 1.35	287.2 0.6	404.9 1.2	486.0 -2.3	553.2 0.76	571.1 0.90	560.7 1.93	495.6 -1.06	413.8 0.96	285.1 -0.84	143.9 0.70	33.1 -7.5
4396 -0.83	35.5 -7.1	150.4 1.30	286.9 -0.69	404.4 -1.34	481.3 -3.2	565.6 -0.62	562.7 -0.58	551.9 0.33	492.0 -1.78	418.1 0.05	288.1 0.24	145.4 1.75	33.4 -6.7

FIG. 21 COMPARISON OF BUNDLE POWERS ALONG CHANNEL L-1 AT 70FPD

ENERGY CLOCK FPD → 5	10	20	25	30	40	50	60	70
1+1+1	4082	4176	4205	4267	4023	4175	3880	4075	4433
1+1+4	4082 0.0	4171 -0.12	4191 -0.33	4252 -0.35	4031 0.2	4166 -0.21	3897 0.44	4073 -0.05	4421 -0.27
1+1+6	4101 0.46	4164 -0.29	4190 -0.33	4243 -0.56	4034 0.27	4135 -0.96	3919 1.00	4065 -0.24	4396 -0.83
2+2+2	4076 -0.15								

FIG. 22 COMPARISON OF CHANNEL L-1 POWERS THROUGHOUT SIMULATION

5	10	20	25	30	40	50	60	70
0.989	1.011	1.054	1.076	1.098	1.141	1.185	1.226	0.328
0.989	1.011	1.054	1.076	1.098	1.141	1.184	1226	0.327
0.989	1.011	1.054	1.076	1.098	1.141	1.184	1.226	0.327
0.989								

FIG. 23 COMPARISON OF CHANNEL L-1 AVERAGE BUNDLE IRRADIATION THROUGHOUT SIMULATION

BUNDLE NUMBER →		1	2	3	4	5	6	7	8	9	10	11	12	13
EP ↓														
1*1*1	4501	39.1	154.1	304.1	430.6	511.2	562.1	576.7	555.9	496.7	404.4	284.1	145.3	37.2
1*1*4	4467 −0.75	36.5 −6.65	156.5 1.56	303.5 −0.20	428.6 −0.46	497.9 −2.6	563.5 0.25	578.4 0.29	564.5 1.55	485.9 −2.17	392.6 −2.92	278.8 −1.86	145.8 0.34	34.4 −7.53
1*1*6	4448 −1.18	37.1 −5.1	159.3 3.37	308.9 1.78	436.2 1.30	509.8 −0.27	578.8 2.97	570.2 −1.13	533.0 −4.12	466.9 −6.0	390.9 −3.34	277.6 −2.29	145.2 −0.07	34.4 −7.23
2*2*2	4584 1.84	36.7 −6.14	157.5 2.21	309.1 1.32	436.5 1.37	510.2 −0.19	579.3 3.06	591.9 2.63	575.1 3.45	499.1 0.48	412.6 2.03	291.3 2.53	150.0 3.25	35.4 −6.84

FIG. 24 COMPARISON OF BUNDLE POWERS ALONG CHANNEL A-14 AT 5FPD

	1	2	3	4	5	6	7	8	9	10	11	12	13
4514	38.3	149.3	292.2	416.3	508.8	564.7	582.1	564.1	506.5	413.8	290.7	148.5	38.1
4496	35.7 −6.79	151.7 1.61	292.4 0.068	415.9 −0.096	499.5 −1.83	569.8 0.90	584.8 0.46	570.9 1.20	496.1 −2.05	407.5 −1.52	287.5 −1.1	149.2 0.47	35.0 −8.13
4489	35.6 −7.05	151.3 1.34	291.6 −0.21	414.8 −0.36	498.2 −2.08	568.2 0.62	580.3 −0.31	563.8 −0.05	494.0 −2.47	412.6 −0.29	291.1 0.14	151.1 1.75	35.5 −6.82

FIG. 25 COMPARISON OF BUNDLE POWERS ALONG CHANNEL A-14 AT 70FPD

ENERGY CLOCK FPD →	5	10	20	25	30	40	50	60	70
1*1*1	4501	4528	4704	4128	4590	4115	4589	4269	4514
1*1*4	4467 −0.75	4498 −0.66	4666 −0.81	4145 0.41	4561 −0.63	4135 0.49	4570 −0.41	4281 0.28	4496 −0.40
1*1*6	4448 −1.18	4470 −1.28	4602 −2.17	4166 0.92	4528 −1.35	4155 0.97	4531 −1.26	4281 0.28	4488 −0.58
2*2*2	4584 1.84								

FIG. 26 COMPARISON OF A-14 CHANNEL POWERS THROUGHOUT SIMULATION

	5	10	20	25	30	40	50	60	70
	0.279	0.304	0.356	0.380	0.402	0.451	0.495	0.544	0.588
	0.279	0.304	0.353	0.379	0.401	0.450	0.494	0.543	0.588
	0.279	0.304	0.353	0.378	0.401	0.449	0.494	0.542	0.586
	0.279								

FIG. 27 COMPARISON OF A-14 CHANNEL AVERAGE BUNDLE IRRADIATION THROUGHOUT SIMULATION

BUNDLE NUMBER

	Σ0 ↓	1	2	3	4	5	6	7	8	9	10	11	12	13
1+1+1	3251	23.7	107.7	222.2	314.1	375.6	406.6	416.3	401.1	364.6	296.0	204.2	99.0	22.3
1+1+4	3258 0.22	21.2 −10.5	108.6 0.83	221.8 −0.18	315.9 0.57	366.7 −2.37	409.3 0.66	420.7 1.54	413.7 3.14	364.6 0.0	293.5 −0.94	202.7 −0.73	99.5 0.51	19.9 −10.8
1+1+6	3241	21.4 −9.7	109.5 1.67	223.6 0.63	318.5 1.40	378.6 0.80	427.6 5.16	417.5 −0.76	389.5 −2.89	348.5 −4.41	289.2 −2.30	199.7 −2.2	98.0 −1.01	19.6 −12.1
2+2+2	3313	21.4 −9.7	109.5 1.67	222.8 0.27	312.0 0.92	373.0 −0.69	417.9 2.78	426.9 2.99	416.9 3.94	370.1 1.51	304.0 2.70	209.9 2.79	103.0 4.94	20.6 −7.6

FIG. 28 COMPARISON OF BUNDLE POWERS ALONG CHANNEL T-23 AT 5FPD

	1	2	3	4	5	6	7	8	9	10	11	12	13
3613	23.4	105.7	222.2	321.7	399.6	448.1	456.1	441.2	399.4	327.8	222.3	104.4	22.9
3474 −0.54	21.1 −9.83	107.5 1.70	221.2 −0.49	323.0 −0831	388.9 −2.68	445.3 −0.50	459.3 0.70	450.2 2.04	397.9 −1.38	319.8 −2.44	219.0 −1.48	105.2 0.77	20.7 −9.6
3448 −1.29	21.3 −8.87	107.4 1.61	220.9 −0.58	321.6 −0.95	389.2 −2.60	446.2 0.70	450.3 −1.27	431.8 −2.13	386.8 −3.65	324.3 −1.868	221.1 −0.09	106.7 2.20	20.9 −8.73

FIG 29 COMPARISON OF BUNDLE POWERS ALONG CHANNEL T-23 AT 70FPD

ENERGY CLOCK
FPD →

	5	10	20	25	30	40	50	60	70
1+1+1	3251	3137	2992	3126	3348	3240	3233	3169	3493
1+1+4	3258 0.22	3145 0.46	3010 0.60	3130 0.13	3345 −0.09	3247 0.216	3235 0.062	3180 0.35	3474 −0.54
1+1+6	3241 −0.31	3155 0.57	3033 1.37	3134 0.26	3339 −0.27	3262	3246 0.40	3195 0.82	3448 −1.29
2+2+2	3313 1.90								

FIG. 30 COMPARISON OF T-23 CHANNEL POWERS THROUGHOUT SIMULATION

5	10	20	25	30	40	50	60	70
1.112	1.129	1.162	1.178	0.288	0.325	0.360	0.395	0.430
1.112	1.129	1.162	1.178	0.288	0.325	0.360	0.395	0.430
1.112	1.129	1.162	1.178	0.288	0.325	0.361	0.396	0.430
1.112								

FIG. 31 COMPARISON OF T-23 CHANNEL AXIAL BUNDLE IRRADIATION THROUGHOUT SIMULATION

BUNDLE NUMBER → / CHANNEL CLEAN ↓		1	2	3	4	5	6	7	8	9	10	11	12	13
1+1+1	0.4011	1.4171	1.335	1.0591	0.648	0.2356	0.0886	0.09126	0.08756	0.08126	0.07183	0.05603	0.02297	0.00824
1+1+4	0.4001	1.4686 −0.017	1.3525 0.019	1.0586 −0.013	0.6671 −0.16	0.2333 −0.98	0.0897 1.24	0.0909 −0.39	0.08963 2.39	0.07934 −2.36	0.07036 −2.05	0.0534 −1.17	0.02982 0.4	0.00792 −3.88
1+1+6	0.4000	1.4170 −0.007	1.3356 0.04	1.0596 0.062	0.648 0.0	0.2345 −0.47	0.0912 2.64	0.0898 1.60	0.0860 −1.76	0.0773 −4.87	0.0703 −2.13	0.0533 1.35	0.0298 0.34	0.00792 −3.88

CORE BURNUP = 10FPD

1+1+1	0.581	1.4376	1.4086	1.1931	0.8267	0.4427	0.3125	0.3126	0.3100	0.2883	0.2554	0.1927	0.1061	0.0295
1+1+4	0.547	1.4363 −0.09	1.4104 0.13	1.1933 0.017	0.8259 −0.097	0.4329 −2.2	0.3187 1.98	0.3208 −0.56	0.3194 3.03	0.2796 −3.02	0.2508 −1.80	0.1907 1.04	0.1070 0.85	0.0279 −5.4
1+1+6	0.546	1.4365 −0.076	1.4111 0.17	1.1944 0.11	0.8235 0.097	0.4358 −1.56	0.3228 3.30	0.3171 −1.70	0.3077 −0.74	0.2730 −5.31	0.2506 −1.88	0.1906 1.09	0.1069 0.75	0.02789 −5.46

CORE BURNUP = 30FPD

1+1+1	0.762	1.4682	1.5183	1.3912	1.0886	0.7404	0.6329	0.6538	0.6294	0.5868	0.5217	0.3959	0.2197	0.0614
1+1+4	0.761	1.4652 −0.20	1.5220 0.24	1.3921 0.065	1.0889 0.017	0.7216 −2.54	0.6470 2.23	0.6505 −0.50	0.6489 3.10	0.5886 −3.1	0.5136 −1.55	0.3919 −1.01	0.2112 0.68	0.0577 −6.03
1+1+6	0.759	1.4652 −0.20	1.5221 0.25	1.3922 0.07	1.0890 0.027	0.7225 −2.08	0.6532 3.21	0.6448 −1.38	0.6314 0.32	0.5596 −4.63	0.5152 −1.25	0.3933 −0.68	0.2119 1.00	0.0579 −5.7

CORE BURNUP = 60 FPD

1+1+1	0.828	1.4779	1.5530	1.4532	1.1696	0.8314	0.7301	0.7543	0.7264	0.6778	0.6033	0.4587	0.2553	0.0715
1+1+4	0.827	1.4746 −0.24	1.5574 0.283	1.4550 0.136	1.1718 0.188	0.8106 −2.5	0.7468 2.29	0.7507 −0.48	0.7490 3.11	0.6573 −3.02	0.5954 −1.311	0.4647 −0.87	0.2571 0.71	0.0671 −6.15
1+1+6	0.826	1.4743 −0.24	1.5570 0.26	1.4544 0.08	1.1709 0.11	0.8169 −1.98	0.7554 3.46	0.7464 −1.05	0.7316 0.74	0.6484 −4.34	0.5873 −0.99	0.4562 −0.54	0.2579 1.02	0.06736 −5.79

CORE BURNUP = 70 FPD

FIG. 32 COMPARISON OF CHANNEL E-14 BUNDLE IRRADIATIONS

	1	2	3	4	5	6	7	8	9	10	11	12	13
0.552	0.03106	0.11256	0.19185	0.23068	0.23825	0.22522	0.20837	0.20474	0.41742	0.90147	1.33117	1.48467	1.43598
0.551	0.03075 −1.0	0.11296 0.355	0.19213 0.15	0.2310 0.18	0.2367 −0.65	0.2269 0.63	0.2084 0.01	0.2065 0.85	0.4160 −0.34	0.9010 −0.052	1.3309 −0.030	1.4945 0.062	1.4356 −0.03
0.552	0.03083 −0.74	0.11323 0.59	0.19261 0.40	0.2315 0.40	0.23785 −0.17	0.2287 1.3	0.2082 −0.06	0.2064 0.06	0.4148 −0.63	0.9006 −0.10	1.3306 −0.043	1.4844 −0.005	1.4356 −0.026

CORE BURNUP = 10FPD

0.687	0.05243	0.1960	0.3358	0.4019	0.4210	0.4595	0.4694	0.4562	0.5933	1.0620	1.4617	1.5591	1.457	
0.687	0.05337 −2.94	0.1980 1.02	0.3370 0.36	0.4056 0.40	0.4125 −2.0	0.4672 1.74	0.4684 −0.21	0.4669 2.2	0.5855 −1.31	1.0592 −0.263	1.4606 −0.089	1.5597 0.038	1.4555 −0.102	
0.687	0.05342 −2.75	0.1982 1.12	0.3373 −0.45	0.4059 0.495	0.4163 −1.12	0.4761 3.18	0.4677 −0.36	0.4587 0.42	0.5809 2.1	1.0585 −0.33	1.4549 −0.123	1.5594 0.02	1.4554 −0.11	

CORE BURNUP = 30FPD

0.887	0.09067	0.31976	0.54699	0.6575	0.6887	0.7450	0.7654	0.7609	0.8549	1.3034	1.6592	1.6723	1.6893	
0.957	0.0871 −3.93	0.3237 1.23	0.5493 0.42	0.6607 0.49	0.6708 −2.60	0.7620 2.28	0.7629 −0.33	0.7621 2.86	0.8371 −7.08	1.2966 −0.52	1.6554 0.37	1.6730 0.062	1.4554 −0.26	
0.886	0.08697 −4.1	0.3232 1.07	0.5484 0.26	0.6596 0.32	0.6760 1.84	0.7727 3.72	0.76125 −0.54	0.7478 0.95	0.8302 −2.81	1.2977 −0.44	1.6563 −0.17	1.6735 0.07	1.4855 −0.25	

CORE BURNUP = 60FPD

0.954	0.10273	0.3611	0.6172	0.7418	0.7777	0.8401	0.8642	0.8359	0.9427	1.3851	1.7262	1.7108	1.5002	
0.953	0.09947 −4.15	0.3557 1.27	0.6199 0.44	0.7457 0.53	0.7568 −2.49	0.8602 2.39	0.8610 −0.37	0.8604 2.93	0.9214 −1.36	1.3769 −0.59	1.7215 −0.27	1.7114 0.055	1.4955 −0.31	
0.953	0.09821 −4.4	0.3547 1.0	0.6183 0.18	0.7438 0.27	0.7621 −2.0	0.8717 3.76	0.8590 −0.60	0.8548 1.06	0.9139 −3.05	1.3785 −0.48	1.7228 −0.20	1.7122 −0.082	1.4957 −0.30	

CORE BURNUP = 70FPD

FIG. 33 COMPARISON OF CHANNEL N-13 BUNDLE IRRADIATIONS

BUNDLE NUMBER → / CHANNEL MEAN ↓	1	2	3	4	5	6	7	8	9	10	11	12	13
1*1*1 1.011	0.08111	0.33594	0.63094	0.87978	1.03962	1.16279	1.19026	1.16154	1.13007	1.27904	1.40161	1.43685	1.40824
1*1*4 1.011	0.08091 −0.25	0.33604 0.03	0.63088 −0.01	0.87978 0.0	1.03861 −0.08	1.16281 0.002	1.19056 0.02	1.16232 0.07	1.12999 −0.01	1.27909 0.004	1.40161 0.0	1.43693 0.006	1.40806 −0.013
1*1*6 1.011	0.08094 0.040	0.33618 0.071	0.63115 0.033	0.88015 0.062	1.03958 0.015	1.16423 0.124	1.19079 0.044	1.16133 0.151	1.12932 −0.067	1.27896 −0.014	1.40145 −0.014	1.43685 0.0	1.40804 −0.0114

CORE BURNUP = 10FPD

1*1*1 1.098	0.09224	0.37759	0.70915	0.98818	1.16885	1.30381	1.33461	1.30135	1.25653	1.38238	1.47389	1.47585	1.41774
1*1*4 1.098	0.09115 −1.18	0.37799 0.11	0.70874 −0.058	0.98801 −0.017	1.16437 −0.38	1.30356 −0.02	1.33575 0.085	1.30497 0.28	1.25580 −0.058	1.38241 0.002	1.47376 −0.009	1.47423 0.026	1.41679 −0.068
1*1*6 1.098	0.09119 −1.14	0.37814 0.146	0.70902 −0.018	0.98840 0.022	1.16764 −0.10	1.30887 0.39	1.33597 0.10	1.30009 −0.097	1.25257 −0.32	1.38152 −0.062	1.47314 −0.051	1.47391 0.004	1.41672 −0.073

CORE BURNUP = 30FPD

1*1*1 1.226	0.10838	0.43359	0.82153	1.14382	1.35489	1.50699	1.56299	1.50364	1.44014	1.53375	1.57996	1.52838	1.42181
1*1*4 1.226	0.10600 −2.19	0.43852 0.21	0.82111 −0.05	1.14436 0.047	1.34443 −0.62	1.50653 0.036	1.54616 0.21	1.5117 0.34	1.4388 −0.093	1.53396 0.046	1.57969 −0.02	1.52903 0.042	1.42963 −0.15
1*1*6 1.226	0.10592 −2.27	0.43821 0.141	0.82052 −0.12	1.14354 −0.024	1.35731 −0.26	1.51661 0.63	1.54702 0.26	1.50447 0.055	1.43413 −0.42	1.53297 −0.021	1.57896 −0.063	1.52865 0.018	1.42954 −0.16

CORE BURNUP = 60FPD

1*1*1 0.328	0.00284	0.01092	0.02080	0.02908	0.03475	0.03792	0.03884	0.03766	0.14697	0.47435	0.85926	1.17979	1.38891
1*1*4 0.327	0.00259 −8.8	0.01096 0.37	0.02089 0.48	0.02946 1.31	0.03395 −2.3	0.03785 −0.185	0.03907 0.59	0.03836 1.86	0.14218 1.92	0.47587 0.24	0.85879 −0.055	1.18065 0.073	1.37949 −0.962
1*1*6 0.327	0.00254 −10.6	0.01076 1.46	0.02051 −1.79	0.02891 0.58	0.03440 −1.01	0.03899 2.82	0.03943 1.52	0.03792 0.69	0.14170 −2.76	0.47572 0.078	0.85768 −0.18	1.17925 −0.046	1.38475 −0.30

CORE BURNUP = 70FPD

NOTE CHANNEL REFUELLED AT 65 FPD

FIG. 34 COMPARISON OF CHANNEL 1-1 BUNDLE IRRADIATIONS

	1	2	3	4	5	6	7	8	9	10	11	12	13
0.304	1.25269	1.06859	0.78682	0.44758	0.14457	0.04806	0.04931	0.04756	0.04256	0.03472	0.02446	0.01254	0.00322
0.304	1.25251 −0.014	1.06855 −0.015	0.78678 0.005	0.44746 −0.032	0.14061 −0.68	0.04816 0.21	0.04963 0.24	0.04819 1.32	0.04177 −1.86	0.03386 −2.48	0.02408 −1.55	0.01258 0.32	0.00301 −6.52
0.304	1.25255 −0.011	1.06874 0.033	0.78714 0.041	0.44796 0.086	0.14147 −0.971	0.04928 2.54	0.04833 −0.97	0.04589 −3.5	0.04039 −5.1	0.03374 −2.82	0.02399 −1.92	0.01253 −0.080	0.00300 −6.83

CORE BURNUP = 10FPD

0.492	1.26313	1.10992	0.96625	0.55671	0.29678	0.20833	0.21619	0.20709	0.18576	0.15202	0.10740	0.05518	0.01418
0.491	1.26279 −0.067	1.11002 0.010	0.96643 0.021	0.55842 −0.052	0.28073 −1.422	0.20931 0.47	0.21681 0.288	0.20964 1.23	0.18203 −2.01	0.14918 −1.87	0.10616 −1.15	0.05562 0.797	0.01318 −7.1
0.491	1.26238 −0.06	1.11041 0.125	0.96718 0.107	0.55769 0.140	0.28253 −0.79	0.21167 1.60	0.21230 −0.882	0.20237 −2.28	0.17764 −4.37	0.14880 −2.12	0.10589 1.406	0.05548 0.54	0.01315 −7.26

CORE BURNUP = 30FPD

0.544	1.27848	1.16959	0.98221	0.72222	0.49055	0.43875	0.45166	0.43765	0.39391	0.32381	0.22799	0.11880	0.03064
0.543	1.27666 −0.14	1.17086 0.194	0.98298 0.078	0.72215 −0.00693	0.48323 −1.49	0.44215 0.715	0.45360 0.429	0.44292 1.294	0.38615 1.97	0.3190 −1.48	0.22764 −1.02	0.11966 0.724	0.02838 −7.37
0.542	1.27673 −0.137	1.17116 0.22	0.98355 0.14	0.72297 0.11	0.48430 −1.27	0.44341 1.06	0.44911 −0.56	0.43291 −1.08	0.38047 −3.41	0.31944 −1.35	0.22795 −0.87	0.11982 0.86	0.02842 −7.24

CORE BURNUP = 60FPD

0.588	1.28343	1.18731	1.01951	0.77509	0.55562	0.51119	0.52620	0.50992	0.45904	0.37755	0.24844	0.13885	0.03585
0.588	1.28133 −0.16	1.19062 0.236	1.02075 0.122	0.77565 0.072	0.54750 −1.46	0.51539 0.82	0.52871 0.48	0.51630 1.25	0.45036 −1.89	0.37243 −1.36	0.24643 −0.90	0.140 0.83	0.03383 −7.31
0.586	1.28138 −0.16	1.19085 0.26	1.02120 0.16	0.77628 0.15	0.54883 −0.68	0.51725 1.18	0.52411 −0.40	0.50924 −0.88	0.44438 −3.19	0.37334 −1.12	0.24669 −0.65	0.14035 1.08	0.03331 −7.89

CORE BURNUP = 70FPD

NOTE CHANNEL REFUELLED AT 4FPD

FIG. 35 COMPARISON OF CHANNEL A-14 BUNDLE IRRADIATIONS

BUNDLE NUMBER → / CHANNEL MEAN ↓	1	2	3	4	5	6	7	8	9	10	11	12	13
1+1 1.129	0.07165	0.36590	0.73367	1.03741	1.22953	1.37942	1.41223	1.37873	1.29373	1.39740	1.48757	1.47057	1.41779
1+4 1.129	0.07247 -0.25	0.36546 0.016	0.73364 -0.004	1.03753 0.011	1.22893 -0.049	1.37960 0.013	1.41267 0.031	1.37959 0.062	1.29373 0.0	1.39773 0.024	1.48747 -0.007	1.47060 0.002	1.41763 -0.011
1+6 1.129	0.07269 -.22	0.36603 0.056	0.73376 0.012	1.0377 0.018	1.22974 0.017	1.38085 0.104	1.41265 0.016	1.37793 -0.058	1.29264 -0.084	1.39744 0.003	1.48727 -0.02	1.47050 -0.005	1.41761 -0.013

CORE BURNUP = 10FPD

1+1 0.288	0.00033	0.00168	0.00306	0.00444	0.00535	0.00588	0.00604	0.00586	0.0842	0.39698	0.79038	1.1151	1.32186
1+4 0.288	0.00030 -9.9	0.00169 0.680	0.00306 0.0	0.00445 1.14	0.00523 -2.24	0.0059 0.34	0.00608 0.66	0.00596 1.31	0.08314 -1.92	0.3974 0.11	0.79063 0.031	1.11646 0.12	1.31911 -0.21
1+6 0.288	0.00029 -12.1	0.00167 -0.67	0.00303 -0.98	0.00439 -23	0.00530 -0.93	0.00607 3.23	0.00615 1.82	0.00594 1.37	0.0833 -1.07	0.3973 0.081	0.7905 0.015	1.11627 0.105	1.32273 0.066

CORE BURNUP = 30FPD

1+1 0.395	0.01006	0.045	0.09373	0.13602	0.16664	0.18425	0.18951	0.18392	0.24439	0.52414	0.87657	1.15623	1.33101
1+4 0.395	0.00917 -9.84	0.04602 2.27	0.09424 0.54	0.13659 0.42	0.16295 -2.2	0.18524 0.54	0.19092 0.74	0.18721 1.79	0.24215 -0.92	0.52423 0.017	0.87665 0.009	1.15816 0.167	1.32737 -0.27
1+6 0.396	0.00916 -8.95	0.04598 2.18	0.09415 0.45	0.13647 0.331	0.16461 -1.22	0.18813 2.10	0.19127 0.928	0.18506 0.62	0.24115 -1.32	0.52482 0.13	0.87697 0.046	1.15820 0.17	1.33104 0.092

CORE BURNUP = 60 FPD

1+1 0.430	0.01316	0.05883	0.12224	0.17751	0.21747	0.24057	0.24761	0.24052	0.29553	0.56512	0.90459	1.16966	1.33401
1+4 0.430	0.01201 -8.74	0.06015 2.39	0.12322 0.67	0.17847 0.54	0.21797 -2.07	0.24210 0.64	0.24841 0.76	0.24466 1.72	0.29285 -0.91	0.56544 0.057	0.90474 0.016	1.1718 0.18	1.33008 -0.29
1+6 0.430	0.01199 -8.89	0.06012 2.19	0.12301 0.50	0.17817 0.37	0.21479 -1.33	0.24538 2.0	0.25028 1.08	0.24297 1.019	0.29122 -1.12	0.56629 0.21	0.90524 0.07	1.17193 0.194	1.33376 -0.019

CORE BURNUP = 70 FPD

NOTE CHANNEL REFUELLED AT 29FPD

FIG. 36 COMPARISON OF CHANNEL T-23 BUNDLE IRRADIATIONS

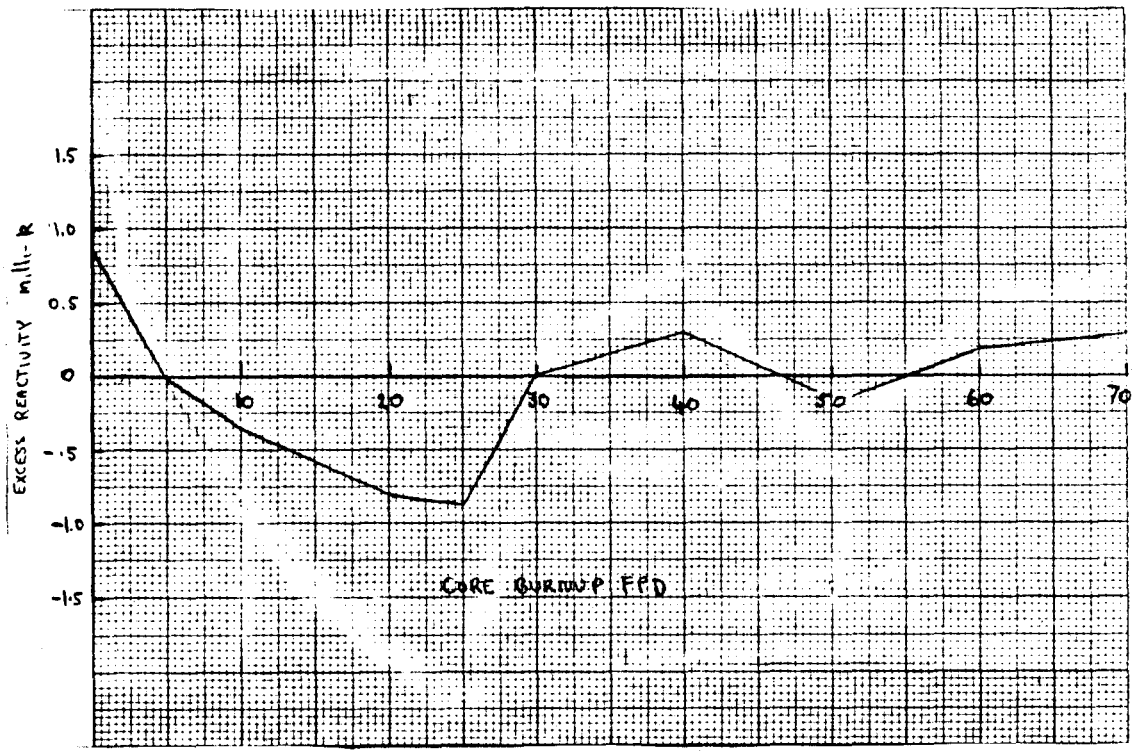

FIG. 37 EXCESS REACTIVITY VS CORE BURNUP

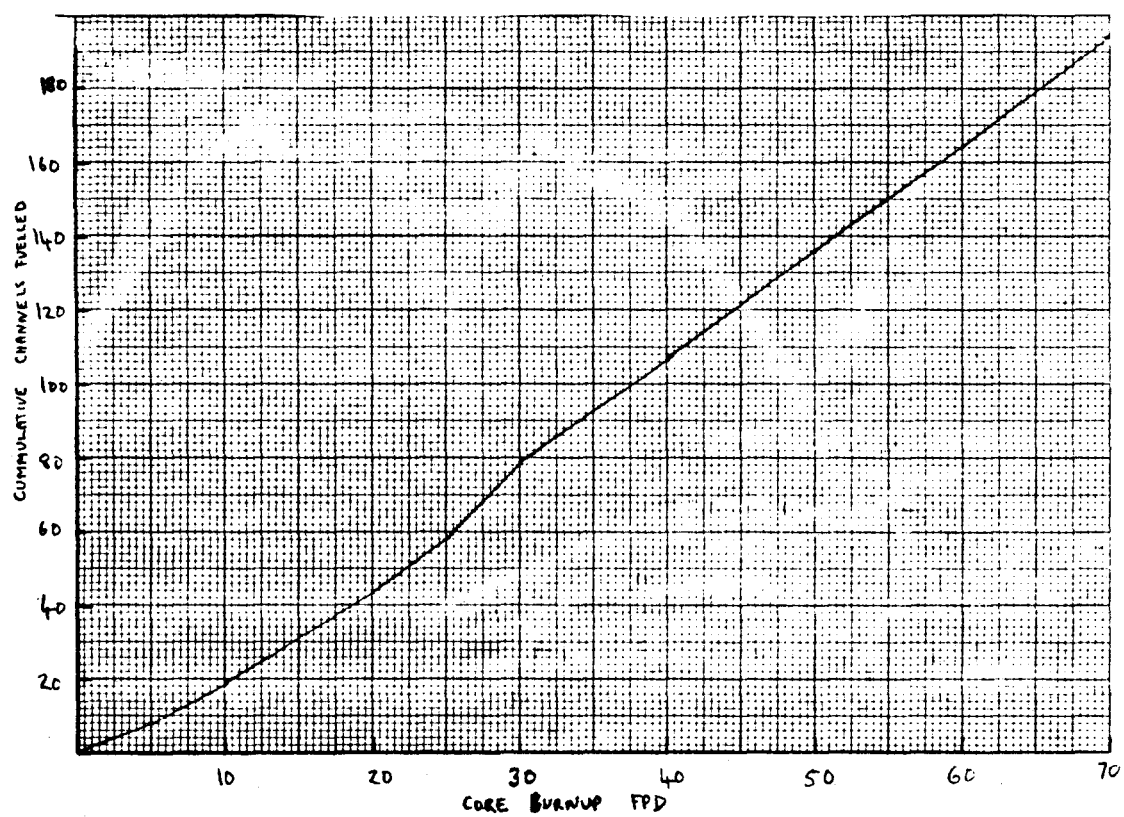

FIG. 38 CUMULATIVE CHANNELS FUELLED VS CORE BURNUP

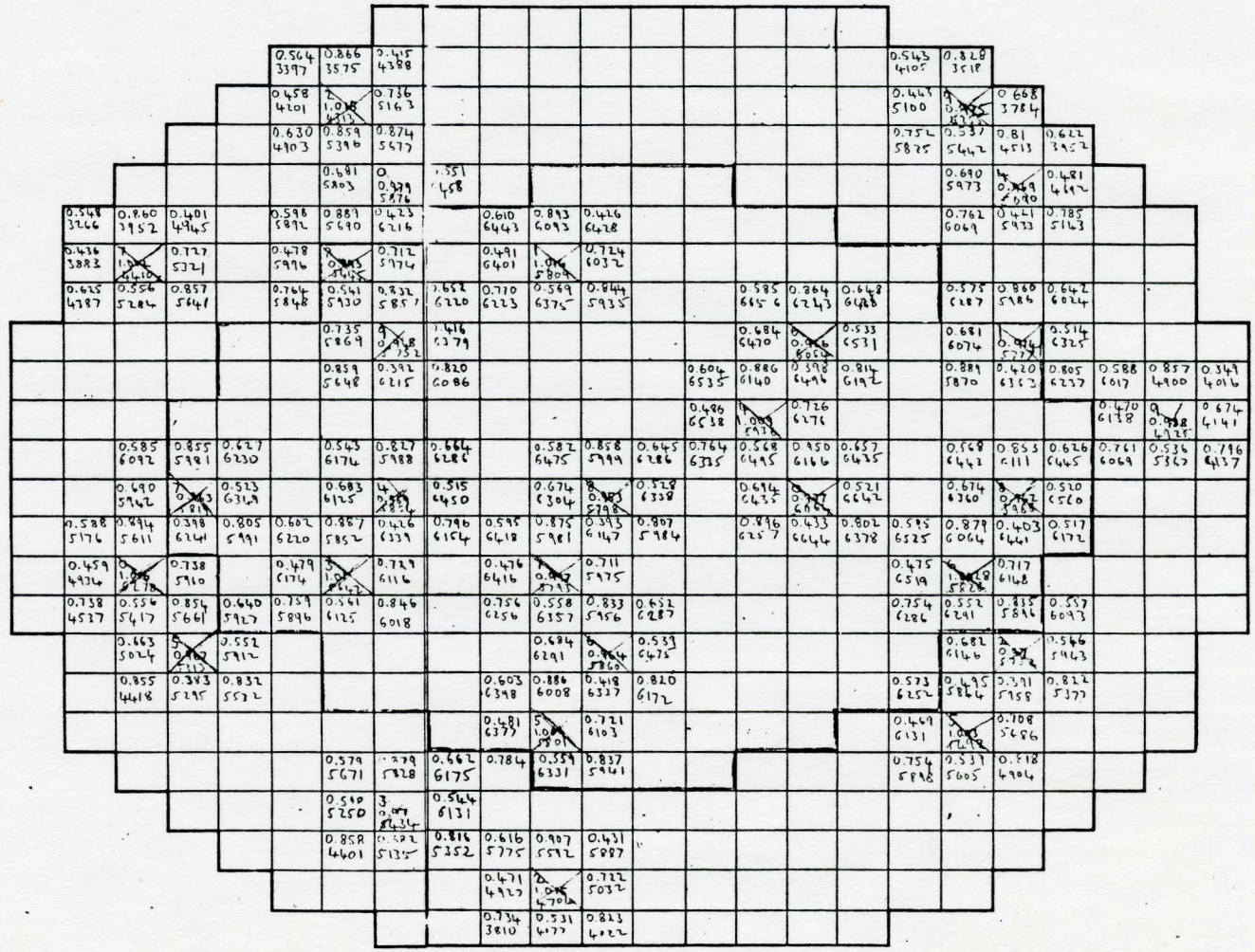

KEY

× AGE AT 30FPD
POWER(Kw) AT 30FPD

CHANNEL REFUELLED AT 30+X FPD

Fig. 39 REACTOR CONDITIONS AT 30FPD AND REFUELLING IN CORE BURNUP INTERVAL 30→40 FPD

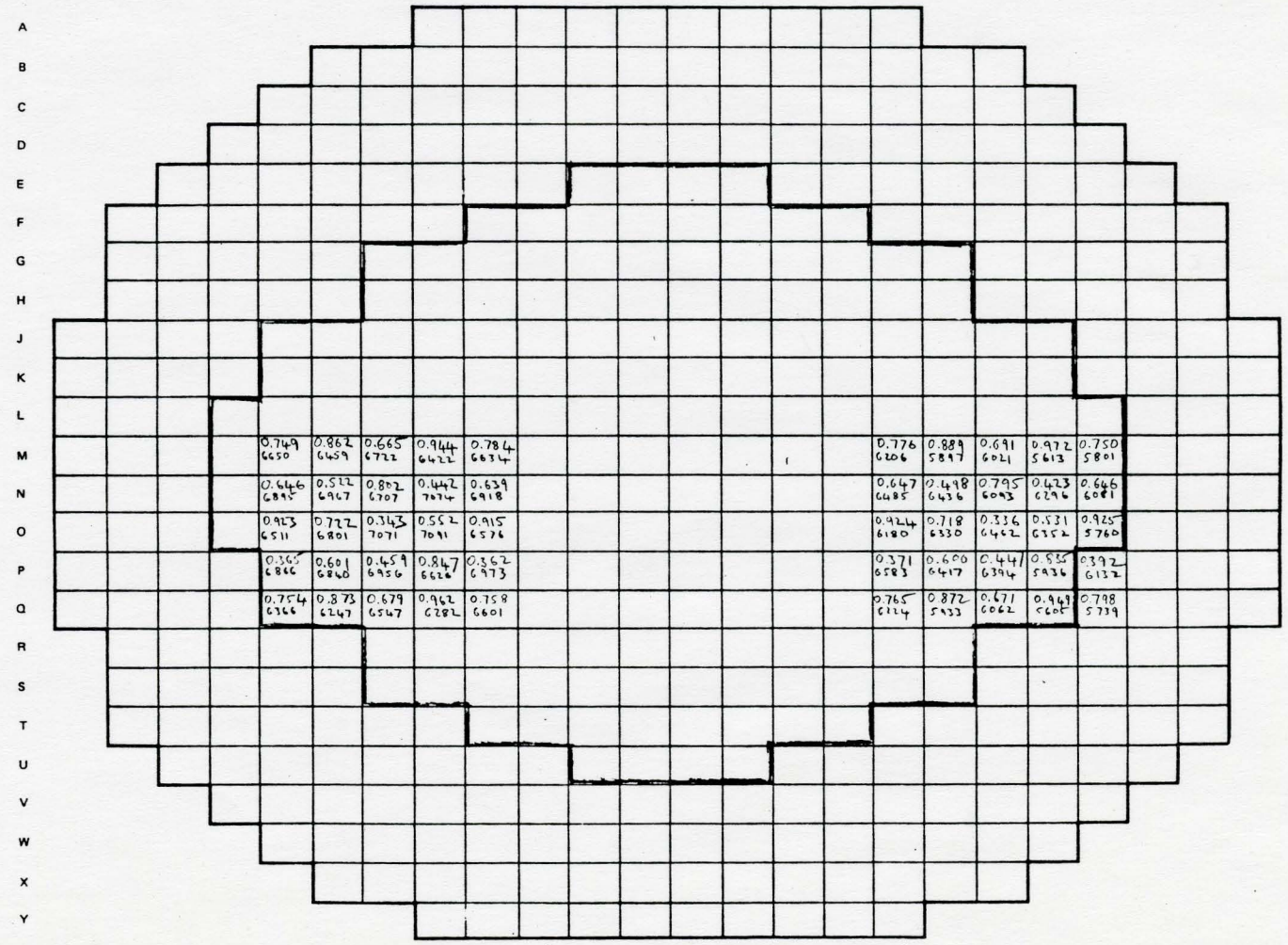

KEY

AGR Power

FIG. 40 REACTOR CONDITIONS ABOUT CHANNELS 0-7 AND 0-19 AT 60FPD

APPENDIX A DESCRIPTION OF CALCULATIONS

The three main types of calculations done in this study are outlined below.

1. Time Averaged Calculations

Flux and power distribtuions are computed using input physics parameters for fuel bundles which are averaged over each bundle's residence time in the core at a given position in the channel. The distributions can be interpreted as an average over a sufficiently long time.

The basic steps are as follows. Note that this is an iterative calculation.

(i) An initial estimate is made of the exit irradiation in the two regions, the size and shape of the inner region, and a starting guess for the axial flux distributions.

(ii) The initial and discharge irradiations for each bundle are computed from the exit irradiation, the axial flux shape, and the fuelling scheme.

(iii) For each position in the channel, average cross sections are calculated by integrating from initial to final irradiation. Figure A.1 illustrates this procedure.

(iv) With these cross sections, the flux distribution, the eigenvalue and the power distribution are calculated.

(v) Steps ii to iv are repeated until the axial flux shape has converged.

(vi) The inner region irradiation is adjusted to get a flat channel power distribution in this region, the outer region irradiation is adjusted to produce the required excess reactivity and the inner region size and shape is adjusted to get the required form factor. All of these factors are not necessarily adjusted at every iteration. Currently this step is done manually.

(vii) Steps ii through v are repeated until the desired form factor and excess reactivity are obtained.

Note that step v is a manual step done externally to the computer so that the job must be resubmitted at each iteration.

2, Instantaneous Calculations

Power distributions which are more representative of those which might be obtained at a particular time during operation are obtained using an instantaneous calculation. This gives a snapshot of the reactor core at a particular moment in the reactor's history. The code assigns each channel in the core an age which represents the time since

the channel was last fuelled as a fraction of its total residence time. These fractions were selected from a uniform random distribution over the interval (0,1) using a numerical random number generator. Knowing the irradiations at the beginning and ending of the dwell period from a time-averaged calculation, the irradiation of each bundle in a channel can be calculated from the fractional age.

A different distribution is produced if a different starting value (the variable NRAN) is used for the random number generator.

The age distribution may also be obtained other than with the random number generator. A fuelling sequence may be read in to produce a patterned distribution of channel ages.

3. Simulations

The time history of the flux and power distribution is calculated at discrete time steps, with the irradiation distribution incremented from the previous step using the previous flux distribution. The flow chart is shown in Fig. A.2.

When a time step is to be taken, the new irradiation for each bundle is calculated from:

$$\omega_K(t_{i+1}) = \omega_K(t_i) + f_K(\omega_i)\, \phi_K \Delta t_i$$

where $\omega(t_i) = \omega_i$ is the previous irradiation
$\omega(t_{i+1})$ is the new irradiation
$f_K(\omega_i)$ is the flux depression factor for the particular bundle
ϕ_K is the bundle flux from the previous time step
Δt_i is the time increment

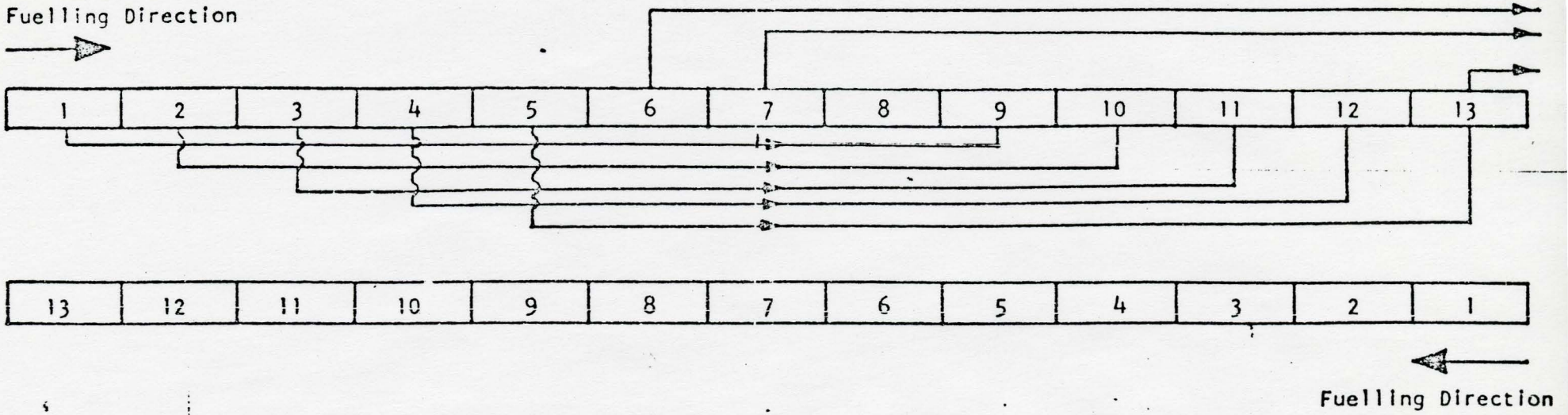

Each channel is

1. Refuelled
2. Is irradiated undisturbed for dwell time T
3. Is refuelled again
4. Bundles are shifted along channel N positions

Irradiation at end of T is:

$$\omega(k) = \omega(k-N) + \int_0^T \phi(k)\,dt$$

$$\bar{\Sigma}(k) = \frac{1}{\Delta\omega(k)} \int_{\omega_1}^{\omega_2} \Sigma(\omega)\,d\omega$$

FIGURE A.1 TIME AVERAGED MODEL

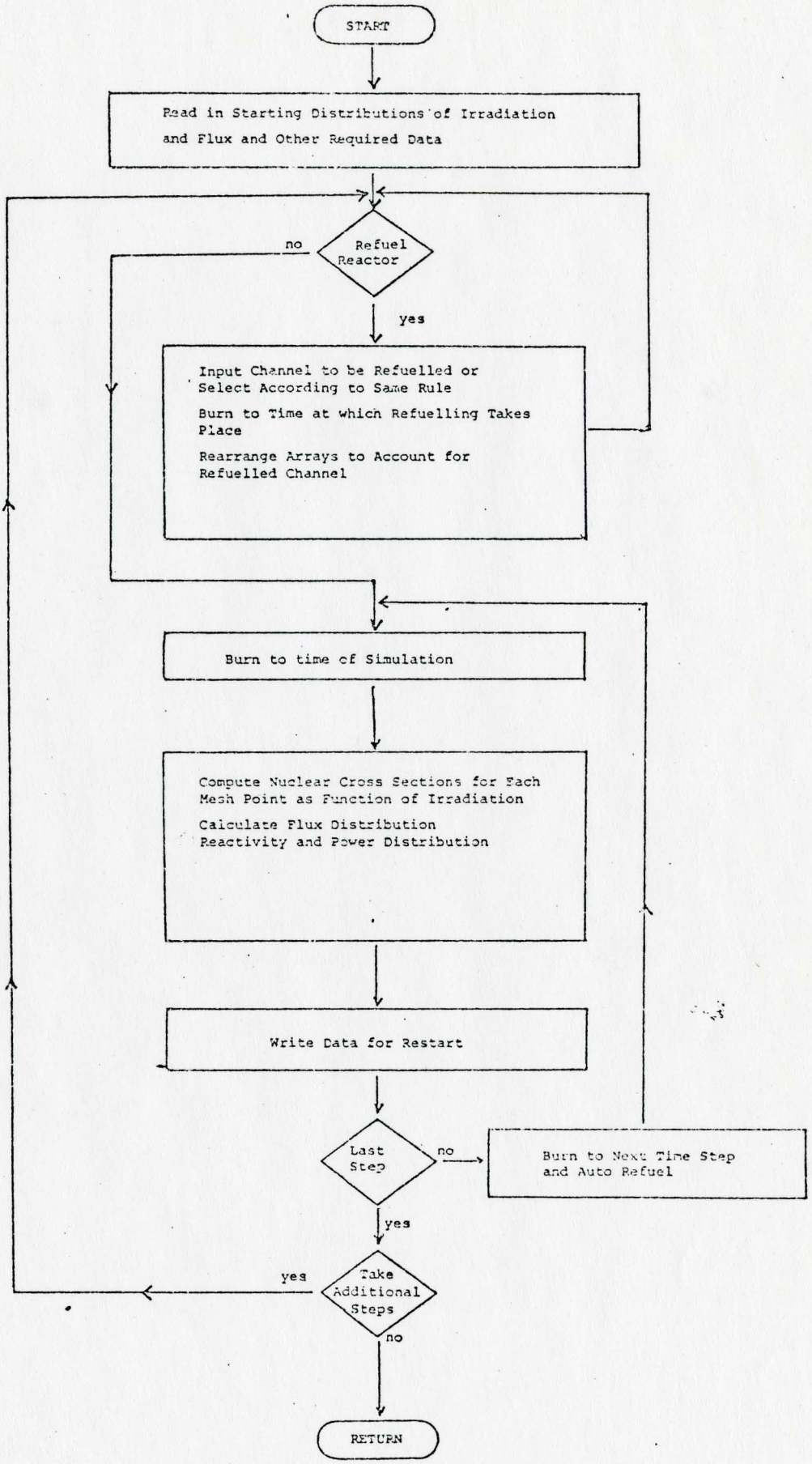

FIGURE A.2 SIMULATION CALCULATION

APPENDIX B REACTOR MODEL

1. Core Model - Mesh and Cell Arrays

For purposes of the flux calculation, the reactor is partitioned by perpendicular mesh planes into small parallelepiped volumes. The flux in each of these volumes is assumed constant, and is assigned to the point at the geometric centre of the volume.

Mesh planes are spaced closely in regions of rapidly changing flux or material properties and farther apart elsewhere.

There is no fixed geometrical relationship between mesh points and bundles. If each bundle is considered to occupy a volume equal to one lattice pitch in the x and y directions and one bundle length in the z direction (called a lattice "cell") the mesh volumes defined by the mesh planes do not necessarily coincide with these cell volumes. There may be more than one mesh point per lattice cell, or one cell may overlap several mesh points.

Mesh arrays are converted to cell arrays by volume weight averaging all mesh point values which overlap each cell. This permits the calculation of the power and burnup of the fuel bundles. These quantities are of most interest in fuel management.

2. Lattice Cell Homogenization

Cross sections for the flux calculation calculated by lattice physics codes (such as POWDERPUFS) are flux-volume weight averaged over the entire volume occupied by the lattice cell. Thus, when more than one mesh point is placed in a physical lattice cell to reduce discretization error in regions of rapidly changing flux, the variation in the flux values of individual mesh points within the geometric region of the cell does not represent the flux distribution through the cell. Rather, the average of the mesh point values is an approximation to the average cell flux. The microscopic flux distribution through the cell is treated by the flux depression factor F.

The material composing the bundle and pressure tubes and moderator are considered to be smeared out uniformly throughout the cell. Thus the model produces power, irradiation, and burnup from mesh points which may be geometrically within the moderator.

When structural material and control elements are present in the region of a lattice cell, appropriate cross section increments are added to the cell cross sections of the affected mesh points. This is to ensure that the total effective number of U, Zr, etc., atoms is unaffected by the introduction of additional material. The displacement of moderator and the change in microscopic flux distribution through the cell, in general non-zero increments will be added to all cross sections. The correct values of increments are obtained from CHEBY "supercell" calculations.

3. Structural Materials and Controllers

Extraneous structural materials, control elements, etc., which are not included in the lattice cell calculation, are treated by adding cross section increments to the cell cross sections at the affected mesh points. Extra materials are considered to be of two types; "fixed" structural material, and "moveable" controllers.

Figure B1 shows how the moveable absorber increments are added to the mesh properties. Consider controller A. It overlaps the mesh volume between I=1 and 2 and J=1 and 2 by 1/3, so that 1/3 of the incremental cross sections of A are added to mesh properties for this mesh point. Similarly for the other mesh volumes overlapped. Thus the increment is smeared over the entire mesh volume. Controller B shows the more normal situation in which the controller occupies the entire mesh volume except at its tip. Controller A is modelled in coarse mesh. Controller B is modelled in fine mesh.

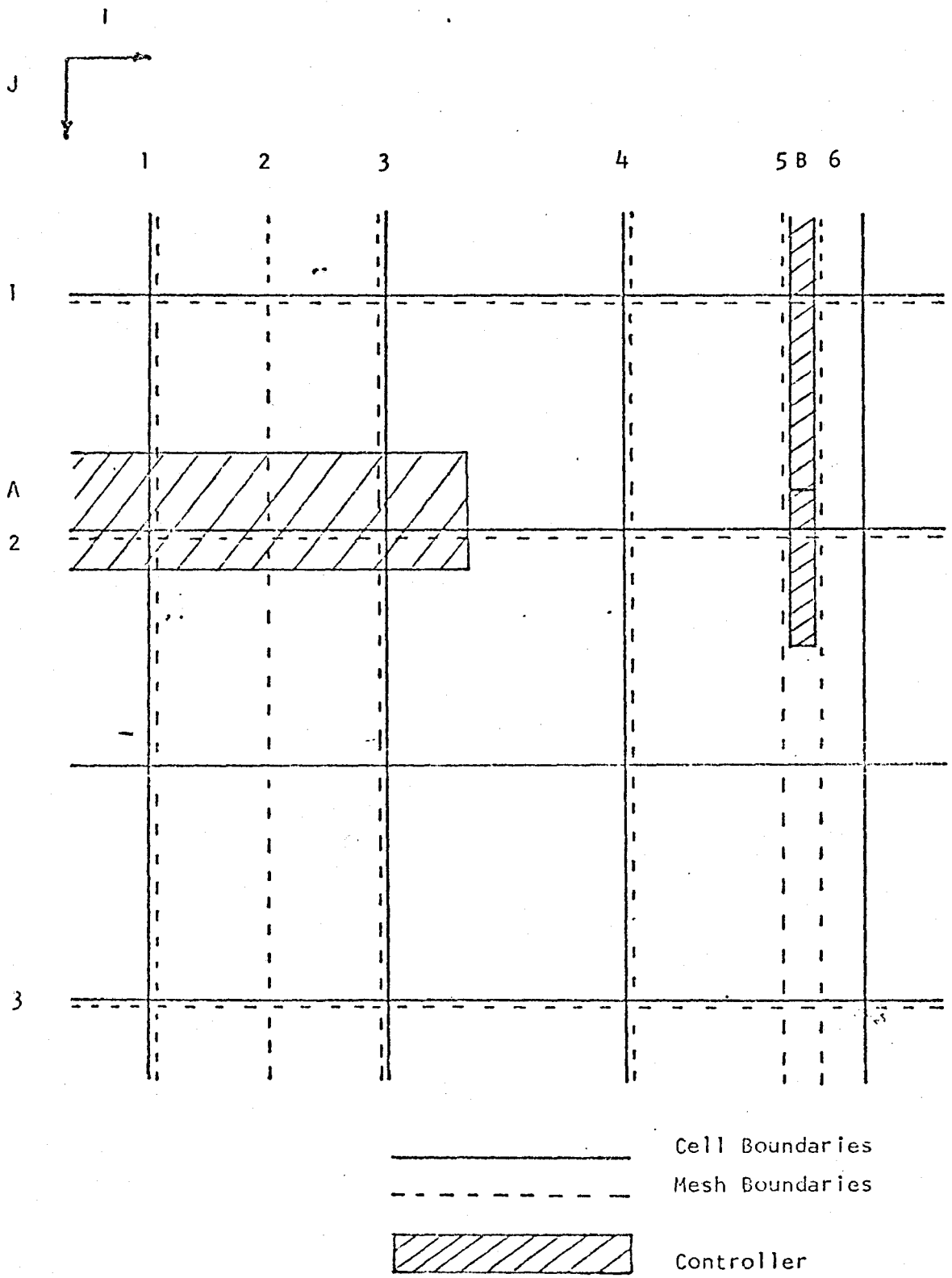

Figure B.1 Mesh and Cell Arrays

APPENDIX C

REFUELLING HISTORY FOR SIMULATION

ENERGY CLOCK FPD	CHANNEL REFUELLED	REGION AND DIRECTION	AVERAGE EXIT IRRADIATION (n/kb)		
				1*1*4	1*1*6
1	V-14	- 0	1.443		
1	W-16	+ 0	1.503		
2	F-16	+ I	1.7781		
2	E-14	- I	1.7167		
3	R-22	- 0	1.448		
3	S-8	+ I	1.7683		
4	B-8	+ 0	1.509		
4	A-14	- 0	1.4668		
5	K-12	+ I	1.800		
5	R-6	- 0	1.467		
5	S-16	+ I	1.799		
6	R-14	- I	1.736		
6	B-16	+ 0	1.516		
7	J-18	- I	1.733		
7	K-4	+ 0	1.5297		
8	J-2	- 0	1.462		
8	W-12	+ 0	1.529		
9	N-14	- I	1.742		
9	F-12	+ I	1.810		
10	K-20	+ I	1.826	1.826	1.826
10	V-10	- 0	1.489	1.489	1.489
10	F-20	+ 0	1.533	1.533	1.533
11	J-10	- I	1.772	1.772	1.773
11	O-16	+ I	1.825	1.825	1.825
12	E-10	- 0	1.502	1.502	1.502
12	O-8	+ I	1.821	1.821	1.821
12	E-18	- 0	1.492	1.492	1.492
13	F-4	+ 0	1.539	1.540	1.540
13	N-22	- 0	1.496	1.496	1.497
14	K-16	+ I	1.829	1.829	1.829
14	V-18	- 0	1.495	1.495	1.496
14	S-12	+ I	1.827	1.827	1.827
15	N-6	- I	1.774	1.774	1.775
15	F-8	+ 0	1.55	1.551	1.551
16	R-10	- I	1.778	1.778	1.779
16	B-12	+ 0	1.55	1.55	1.55
16	J-14	- I	1.776	1.777	1.777
17	O-20	+ I	1.84	1.844	1.844
17	E-22	- 0	1.46	1.460	1.461
18	O-4	+ I	1.850	1.850	1.850
18	N-2	- 0	1.502	1.503	1.503
19	O-24	+ 0	1.551	1.552	1.552
19	A-10	- 0	1.482	1.483	1.483
20	S-20	+ 0	1.565		
20	E-6	- 0	1.513		
20	W-8	+ 0	1.566		
21	N-10	- I	1.794		
21	S-4	+ 0	1.570		
21	V-6	- 0	1.507		
22	O-12	+ I	1.86		
22	J-22	- 0	1.515		
22	K-8	+ I	1.853		
23	R-18	- I	1.797		
23	W-20	+ 0	1.560		
23	J-6	- I	1.787		
24	K-24	+ 0	1.542		
24	R-2	- 0	1.501		
24	T-15	+ I	1.787		
25	N-18	- I	1.832		
25	T-17	+ 0	1.533		
25	E-16	- 0	1.491		
25	C-15	+ 0	1.53		
26	R-8	- I	1.732		
26	G-15	+ I	1.812		
26	R-16	- I	1.728		
26	V-16	- 0	1.491		
27	L-3	+ 0	1.538		
27	L-11	+ I	1.805		
27	J-12	- I	1.725		
27	P-15	+ I	1.792		
28	V-12	- 0	1.484		
28	G-19	+ 0	1.535		
28	J-4	- 0	1.484		
28	X-15	+ 0	1.533		
29	E-12	- I	1.732		
29	L-19	+ I	1.803		
29	T-23	+ 0	1.473		
29	C-11	+ 0	1.53		
30	E-8	- 0	1.468		
30	P-3	+ 0	1.524		
30	N-16	- I	1.739		
31	G-11	+ I	1.815		
31	J-20	- I	1.74		
32	X-11	+ 0	1.535		
32	R-20	- 0	1.468		
32	C-7	+ 0	1.533		
33	V-8	- 0	1.474		
33	P-7	+ I	1.82		
34	E-20	- 0	1.49		
34	L-15	+ I	1.824		
34	N-8	- I	1.752		
35	T-11	+ I	1.829		
35	R-4	- 0	1.48		
35	T-19	+ 0	1.538		
36	J-16	- I	1.76		
36	P-19	+ I	1.826		
36	R-12	- I	1.758		
37	G-3	+ 0	1.54		
37	N-4	- I	1.76		
37	P-11	+ I	1.822		

APPENDIX C - continued

ENERGY CLOCK FPD	CHANNEL REFUELLED	REGION AND DIRECTION	AVERAGE EXIT IRRADIATION (n/kb)		
38	N-20	- I	1.768		
38	G-7	+ I	1.819		
38	N-12	- I	1.75		
39	L-23	+ 0	1.535		
39	J-8	- I	1.747		
39	C-19	+ 0	1.51		
40	V-20	- 0	1.470		
40	P-23	+ 0	1.563		
40	A-16	- 0	1.465		
41	L-7	+ I	1.827		
41	N-24	- 0	1.460		
41	G-23	+ 0	1.501		
42	A-12	- 0	1.465		
42	C-13	+ 0	1.512		
42	F-15	- I	1.71		
43	G-13	+ I	1.76		
43	S-15	- I	1.71		
43	L-9	+ I	1.76		
44	A-8	- 0	1.467		
44	X-19	+ 0	1.512		
44	W-15	- 0	1.477		
45	T-3	+ 0	1.52		
45	V-4	- 0	1.461		
45	X-7	+ 0	1.508		
46	K-11	- I	1.718		
46	X-13	+ 0	1.507		
46	F-19	- 0	1.47		
47	T-17	+ 0	1.52		
47	J-24	- 0	1.44		
47	G-5	+ 0	1.504		
48	O-15	- I	1.73		
48	C-9	+ 0	1.508		
48	S-7	- I	1.72		
49	L-17	+ I	1.62		
49	K-19	- I	1.71		
49	L-5	+ I	1.75		
				1*1*4	1*1*6
50	E-4	- 0	1.518	1.519	1.521
50	P-21	+ 0	1.561	1.564	1.565
50	K-3	- 0	1.497	1.498	1.499
50	T-23	+ I	1.810	1.811	1.811
51	F-11	- I	1.736	1.738	1.739
51	G-17	+ I	1.802	1.804	1.803
51	W-11	- 0	1.497	1.499	1.501
52	G-9	+ I	1.808	1.810	1.810
52	F-7	- 0	1.480	1.482	1.484
52	T-5	+ 0	1.553	1.555	1.556
53	O-3	- 0	1.497	1.498	1.500
53	T-21	+ 0	1.530	1.531	1.532
53	B-15	- 0	1.476	1.477	1.478
54	P-13	+ I	1.814	1.815	1.815
54	S-19	- 0	1.483	1.485	1.488
54	P-5	+ I	1.812	1.814	1.815

ENERGY CLOCK FPD	CHANNEL REFUELLED	REGION AND DIRECTION	AVERAGE EXIT IRRADIATION (n/kb)		
55	K-15	- I	1.754	1.757	1.757
55	P-17	+ I	1.820	1.821	1.821
56	S-11	- I	1.756	1.759	1.761
56	G-21	+ 0	1.543	1.544	1.544
56	O-7	- I	1.766	1.762	1.764
57	L-13	+ I	1.830	1.830	1.830
57	O-19	- I	1.755	1.757	1.760
57	T-9	+ I	1.824	1.826	1.827
58	O-11	- I	1.750	1.753	1.754
58	C-17	+ 0	1.544	1.544	1.544
59	K-7	- I	1.724	1.726	1.727
59	P-9	+ I	1.833	1.835	1.835
60	O-23	- 0	1.498	1.499	1.502
60	L-21	+ I	1.830	1.833	1.833
61	B-11	- 0	1.502	1.503	1.504
61	D-16	+ 0	1.540	1.540	1.539
61	F-17	- 0	1.473	1.475	1.475
62	U-16	+ 0	1.544	1.546	1.546
62	K-23	- 0	1.469	1.470	1.472
62	X-9	+ 0	1.538	1.539	1.541
63	W-13	- 0	1.463	1.466	1.468
63	U-8	+ 0	1.537	1.538	1.540
63	S-5	- 0	1.460	1.465	1.465
64	D-12	+ 0	1.542	1.542	1.542
64	W-7	- 0	1.460	1.462	1.465
64	D-8	+ 0	1.534	1.535	1.537
64	S-23	- 0	1.451	1.452	1.454
65	L-1	+ 0	1.532	1.533	1.533
65	W-19	- 0	1.457	1.459	1.461
65	H-20	+ 0	1.527	1.530	1.530
				1*1*4	1*1*6
66	K-9	- I	1.713	1.716	1.717
66	H-4	+ 0	1.523	1.524	1.524
66	F-13	- I	1.708	1.711	1.711
67	Q-4	+ 0	1.529	1.531	1.532
67	K-17	- I	1.711	1.714	1.714
67	M-12	+ I	1.781	1.781	1.781
68	S-17	- I	1.673	1.675	1.677
68	H-16	+ I	1.803	1.804	1.804
68	K-5	- I	1.661	1.663	1.663
69	Q-20	+ I	1.747	1.750	1.752
69	S-21	- 0	1.460	1.471	1.474
69	M-4	+ I	1.8002	1.802	1.8023

Note: About the first 27 oldest channels at 0 FPD are fuelled in the positive direction. This is a peculiarity of the particular starting pattern selected. Throughout the simulation, average discharge irradiations for channels fuelled positively generally exceeded the time-averaged value, while the value for channels fuelled negatively was generally lower than the time-averaged value.